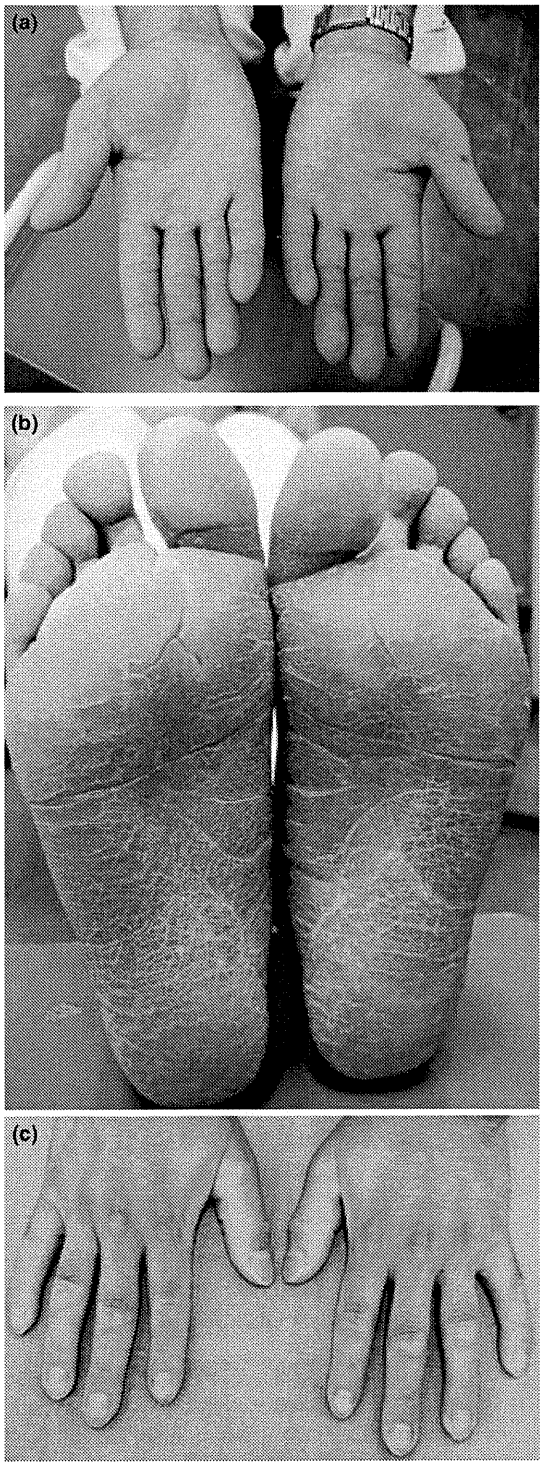

Figure 1. Diffuse hyperkeratosis of the bilateral palms and soles with a yellowish discoloration (a,b). Clinical findings of the dorsal aspect of the hand. Keratotic erythema is evenly spread on the distal portion of the dorsal aspect of the finger. The knuckle pads of the right index and middle finger and the border of the keratotic erythema are continuous (c).

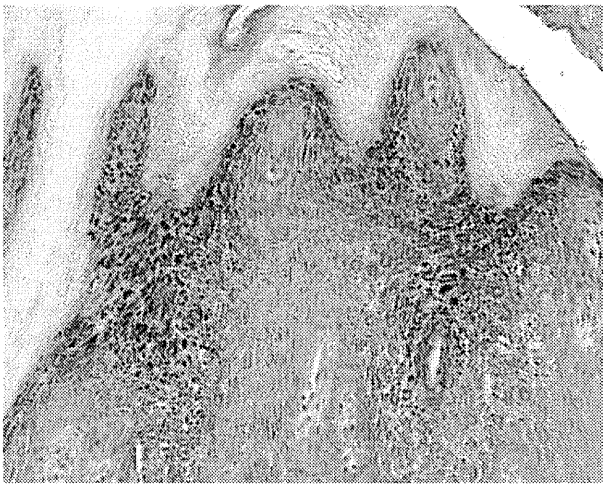

Figure 2. Histopathology of a skin biopsy from the palm. Marked hyperkeratosis, acanthosis and hypergranulosis are observed. A coarse aggregated granule in the granular layer and vacuolar changes in the spinous layer are also seen (hematoxylin–eosin, original magnification ×200).

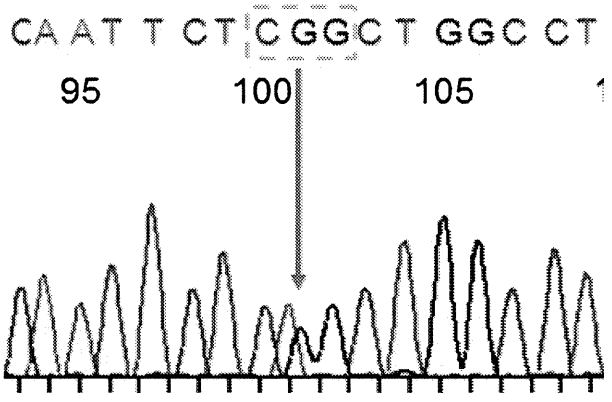

Figure 3. A heterozygous missense mutation c.488G>A in exon 1 leading to p.R163Q was detected.

conserved regions at the beginning of 1A and at the end of 2B, which are termed the helix initiation motif (HIM) and the helix termination motif (HTM), respectively.[13] They play very important roles to maintain the structure of the keratin intermediate filaments. *KRT 9* mutations are predominantly involved in the HIM region, which is considered to be crucial for keratin heterodimerization.[14] Mutant K9 weakens the cytoskeleton, and excessive hyperkeratosis occurs in response to mechanical friction.

We have summarized the cases of EPPK with knuckle pads and documented *KRT 9* mutations

Table 1. Summary of EPPK with knuckle pads and detected *KRT 9* mutation

No	Age at the consultation	Sex	*KRT 9* mutation, nucleotide change	Amino acid change	Ethnicity	Reference
1	–	–	c. 478C>T	p. L160F	Chinease	7
2	42	M	c. 482A>T	p. N161I	Not described	8
3	13	M	c. 482A>G	p. N161S	Japanese	9
4	–	–	c. 487C>T	p. R163W	Taiwanese	10
5	–	–	c. 487C>T	p. R163W	Italian	12
7	26	M	c. 488G>A	p. R163Q	Japanese	Present case
6	33	M	c. 503T>C	p. L168S	Chinease	11

EPPK, epidermolytic palmoplantar keratoderma; *KRT9*, Keratin 9 gene.

(Table 1).[7–12] All of these mutations are located in the HIM region, and no correlation with ethnicity has been seen. Although the R163Q mutation of *KRT 9* in our case is a recurrent mutation,[2] this is the first case of this mutation with knuckle pads in EPPK. While Lu *et al.*[7] suggested that mutation of *KRT 9* might be the cause of the knuckle pads, no obvious genotype and phenotype correlation has been found to date.

Codispoti *et al.*[12] revealed that the amount of K9 mRNA expression in the knuckle pads of an EPPK patient was elevated approximately 90-fold compared with that in non-EPPK individuals and suggested the ectopic expression of K9 in the proximal interphalangeal and metacarpophalangeal joints. Our patient had keratotic erythema around the knuckle pads and on the distal dorsal aspect of the fingers. We also speculated that our case may have developed the knuckle pads and keratotic erythema due to ectopic mutant K9 expression and repetitive mechanical friction. Recently, Funakushi *et al.*[15] reported an EPPK case with pseudoainhum-like constriction bands and keratotic erythema similar to our case. The border of K9 expression may vary depending on the individual and lead to distinctive clinical features.

In summary, this is the first case of an R163Q mutation in *KRT 9* in an EPPK patient with knuckle pads and our case expands the database of EPPK patients with knuckle pads. In addition, our case also showed a unique distribution of keratotic erythema on the fingers. We could not analyze the knuckle pads histologically; however, we speculated that the existence of ectopic mutant K9 and mechanical friction led to the formation of the knuckle pads and keratotic erythema.

Masahiro HAYASHI,[1] Hajime NAKANO,[2]
Daisuke SAWAMURA,[2] Tamio SUZUKI[1]
[1]*Department of Dermatology, Yamagata University School of Medicine, Yamagata, and* [2]*Department of Dermatology, Hirosaki University School of Medicine, Hirosaki, Japan*

REFERENCES

1 Vörner H. Zur Kenntnis des Keratoma hereditarium palmare et plantare. *Arch Dermatol Syph* 1901; **56**: 3–31.
2 Reis A, Hennies HC, Langbein L *et al.* Keratin 9 gene mutations in epidermolytic palmoplantar keratoderma (EPPK). *Nat Genet* 1994; **6**: 174–179.
3 Knapp AC, Franke WW, Heid H, Hatzfeld M, Jorcano JL, Moll R. Cytokeratin No. 9, an epidermal type I keratin characteristic of a special program of keratinocyte differentiation displaying body site specificity. *J Cell Biol* 1986; **103**: 657–667.
4 Moll R, Franke WW, Schiller DL, Geiger B, Krepler R. The catalog of human cytokeratins: patterns of expression in normal epithelia, tumors and cultured cells. *Cell* 1982; **31**: 11–24.
5 Kobayashi S, Tanaka T, Matsuyoshi N, Imamura S. Keratin 9 point mutation in the pedigree of epidermolytic hereditary palmoplantar keratoderma perturbs keratin intermediate filament network formation. *FEBS Lett* 1996; **386**: 149–155.
6 Swensson O, Langbein L, McMillan JR *et al.* Specialized keratin expression pattern in human ridged skin as an adaptation to high physical stress. *Br J Dermatol* 1998; **139**: 767–775.
7 Lu Y, Guo C, Liu Q *et al.* A novel mutation of keratin 9 in epidermolytic palmoplantar keratoderma combined with knuckle pads. *Am J Med Genet A* 2003; **120A**: 345–349.
8 Küster W, Reis A, Hennies HC. Epidermolytic palmoplantar keratoderma of Vörner: re-evaluation of Vörner's original family and identification of a novel keratin 9 mutation. *Arch Dermatol Res* 2002; **294**: 268–272.
9 Hamada T, Ishii N, Karashima T, Kawano Y, Yasumoto S, Hashimoto T. The common *KRT9* gene mutation in a

Japanese patient with epidermolytic palmoplantar keratoderma and knuckle pad-like keratoses. *J Dermatol* 2005; **32**: 500–502.
10 Chiu HC, Jee SH, Sheen YS, Chu CY, Lin PJ, Liaw SH. Mutation of keratin 9 (R163W) in a family with epidermolytic palmoplantar keratoderma and knuckle pads. *J Dermatol Sci* 2007; **45**: 63–65.
11 Li M, Yang LJ, Hua HK, Zhu XH, Dai XY. Keratin-9 gene mutation in epidermolytic palmoplantar keratoderma combined with knuckle pads in a large Chinese family. *Clin Exp Dermatol* 2009; **34**: 26–28.
12 Codispoti A, Colombo E, Zocchi L *et al.* Knuckle pads, in an epidermal palmoplantar keratoderma patient with Keratin 9 R163W transgrediens expression. *Eur J Dermatol* 2009; **19**: 114–118.
13 Lu X, Lane EB. Retrovirus-mediated transgenic keratin expression in cultured fibroblasts: specific domain functions in keratin stabilization and filament formation. *Cell* 1990; **62**: 681–696.
14 Rothnagel JA, Wojcik S, Liefer KM *et al.* Mutations in the 1A domain of keratin 9 in patients with epidermolytic palmoplantar keratoderma. *J Invest Dermatol* 1995; **104**: 430–433.
15 Funakushi N, Mayuzumi N, Sugimura R *et al.* Epidermolytic palmoplantar keratoderma with constriction bands on bilateral fifth toes. *Arch Dermatol* 2009; **145**: 609–610.

Novel mutation of the *KRT 10* gene in a Japanese patient with epidermolytic hyperkeratosis

Dear Editor,

Epidermolytic hyperkeratosis (EH; Online Mendelian Inheritance in Man 113800), also known as bullous congenital ichthyosiform erythroderma or epidermolytic ichthyosis, is a rare autosomal dominant skin disease characterized by generalized erythrodermic ichthyosiform skin, and is caused by mutations in the genes that encode either Keratin 1 or Keratin 10.[1] This report describes a novel mutation in the 2B region of the *KRT 10* gene that was detected in a Japanese patient with EH.

A 44-year-old woman consulted our department for the evaluation of skin lesions. She had been diagnosed with EH based on a histological analysis at the age of 13 years. Her parents and siblings were unaffected. A physical examination revealed generalized erythrodermic ichthyosiform skin and areas of erosive skin, especially at flexures without involvement of the palms, soles, hair, nails or mucosa (Fig. 1a). A histological finding showed marked hyperkeratosis and granular degeneration with acanthosis from the upper spinous to granular layers (Fig. 1b). We performed a sequence analysis of the *KRT 10* gene in a peripheral blood sample after obtaining the patient's informed consent. A heterozygous substitution (c. T1345G) was identified in exon 6 of the *KRT 10* gene (Fig. 2a). This exchange resulted in a substitution of a tyrosine residue (TAC) by an arginine residue (GAC) at codon 449 (p.Y449D). This mutation was confirmed by electrophoresis using the restriction enzyme BsiEI-digested polymerase chain reaction products from exon 6, because the substitution in the *KRT 10* gene of this case creates a BsiEI recognition site in the mutant allele (Fig. 2b). This mutation has never been reported to date and was not found in 100 normal unrelated alleles. It is possible that the absence of palmoplantar involvement was associated with this particular mutation of *KRT 10*.

Epidermolytic hyperkeratosis is a dominantly inherited disorder caused by a *KRT 1* or *KRT 10* gene mutation. This report identified a novel missense mutation, p.Y449D, in the *KRT 10* gene. This affected the 2B region of Keratin 10, where many other missense mutations associated with EH have been reported. Most keratin mutations associated with hereditary skin diseases affect residues at the end of the rod domain of the keratin proteins, and the p.Y449D mutation in this patient is consistent with that observation.

Correspondence: Teruhiko Makino, M.D., Ph.D., Department of Dermatology, Graduate School of Medicine and Pharmaceutical Sciences, University of Toyama, 2630 Sugitani, Toyama 930-0194, Japan. Email: tmakino@med.u-toyama.ac.jp
Conflict of interest: The authors have no conflict of interest to disclose.
Funding sources: The authors have no funding sources which supported this work.

Correspondence

Possible modifier effects of keratin 17 gene mutation on keratitis–ichthyosis–deafness syndrome

DOI: 10.1111/j.1365-2133.2011.10696.x

Madam, Keratitis–ichthyosis–deafness (KID) syndrome (OMIM 148210, 242150) is a rare type of ectodermal dysplasia caused by mutations in the gap junction protein beta-2 gene (*GJB2*)[1] or beta-6 gene (*GJB6*).[2] On the other hand, mutations in genes encoding keratin 6a, 6b, 16 and 17 (*KRT6A*, *KRT6B*, *KRT16* and *KRT17*) are known to cause pachyonychia congenita (PC; OMIM 16720, 17210). PC and KID syndrome share similar symptoms, such as palmoplantar hyperkeratosis and onychodystrophy. This study reports a Japanese patient with atypical KID syndrome with the combined heterozygous mutations of a recurrent mutation in *GJB2* and a novel mutation in the V1 region of *KRT17*.

The proband was a 40-year-old Japanese woman. She was the child of healthy, nonconsanguineous parents. From childhood, she had shown diffuse mutilating palmoplantar hyperkeratosis (Fig. 1a), nail dystrophy (Fig. 1b), hypotrichosis, sensorineural hearing loss, and vascularized keratitis. Periorificial hyperkeratosis was not seen. From these findings, the diagnosis of KID syndrome was made. She had had recurrent bacterial and fungal skin infections. In her twenties, painful tumours appeared on her lower limbs. In her thirties, tumours on both buttocks developed to take on a papilloma-like appearance (Fig. 1c). Etretinate with topical or systemic antibiotics and antifungal agents did not alleviate her symptoms. Skin abrasion was repeatedly conducted on the tumours. Histopathology of the lesions revealed epidermal pseudocarcinomatous hyperplasia with dilation of vessels in papillary and reticular dermis accompanied by mixed immune cell infiltrates, excluding the involvement of squamous cell carcinoma (Fig. 1d). Vacuolated keratinocytes, suggesting human papillomavirus infection, were not detected.

Genomic DNA extracted from peripheral blood was used as a template for polymerase chain reaction (PCR) amplification. Direct sequencing of *GJB2*, *GJB6*, *KRT6A*, *KRT6B*, *KRT16* and *KRT17* was performed as described elsewhere.[3–5] The medical ethical committee of Hokkaido University approved all the described studies. The study was conducted according to the Declaration of Helsinki Principles. The proband gave her written informed consent.

Mutation analysis of the proband's genomic DNA revealed a c.148G>A transition (p.Asp50Asn) in *GJB2* (Fig. 2a), which is the most prevalent mutation in patients with KID syndrome.[1] Furthermore, the proband was found to be heterozygous for a c.177C>A transversion (p.Ser59Arg) in *KRT17* (Fig. 2b). Restriction enzyme digestion of the PCR products by PvuII was carried out to confirm the c.177C>A in *KRT17* (Fig. 2c). The c.177C>A in *KRT17* was novel and was not detected in 200 alleles from 100 normal Japanese individuals. Mutation screening on the proband's parents could not be performed because the father was not alive and the mother did not consent. Keratin 17 (K17) immunohistochemistry on skin samples from several different sites revealed K17 expression in whole epidermis although its expression level did not vary between nonlesional and lesional skin specimens (data not shown).

As the clinical manifestations of the proband were atypical and more severe than those of other patients with KID syndrome – as evidenced, for example, by diffuse mutilating palmoplantar hyperkeratosis and recurrent granulation tissue formation on the buttock – we hypothesized that mutations in other genes might have affected the proband's phenotype through modifier effects. Modifier genes are defined as genes that affect the phenotypic expression of another gene, and several studies have demonstrated that modifier genes are involved in manifestations of inherited disorders.[6] *KRT6A*, *KRT6B*, *KRT16* and *KRT17*, the causative genes of PC, which affects the nails and the palmoplantar area, were selected as candidates for modifier gene investigation in our case, although we cannot exclude the possibility that there are some other genes which modify KID syndrome phenotype.

Most of the keratin mutations are within the helix boundary motifs, which are crucial for keratin monomers to form dimers and subsequent keratin networks.[7] The *KRT17* mutation found in the proband was located not within the helix boundary motifs but in the V1 region of K17 (Fig. 2d). In other keratin genes, such as *KRT5* and *KRT16*, some mutations have been reported within the V1 region, and the phenotypes resulting from these mutations are milder than those resulting from the mutations within the helix boundary motifs.[7] The V1 regions of keratin intermediate filament have glycine loops[8] and it has been suggested that these structures modulate flexibility and other unknown physical attributes of keratin filaments by interacting with similar structures in loricrin.[9] Ser^{59} is located within a highly conserved segment composed of the glycine loop in K17 (Fig. 2e). p.Ser59Arg in K17 is predicted to be probably damaging by PolyPhen-2, with a score of 0·893.[10]

Based on these findings, it is conceivable that the p.Ser59-Arg variant in K17 has a modifying effect on the pathogenic

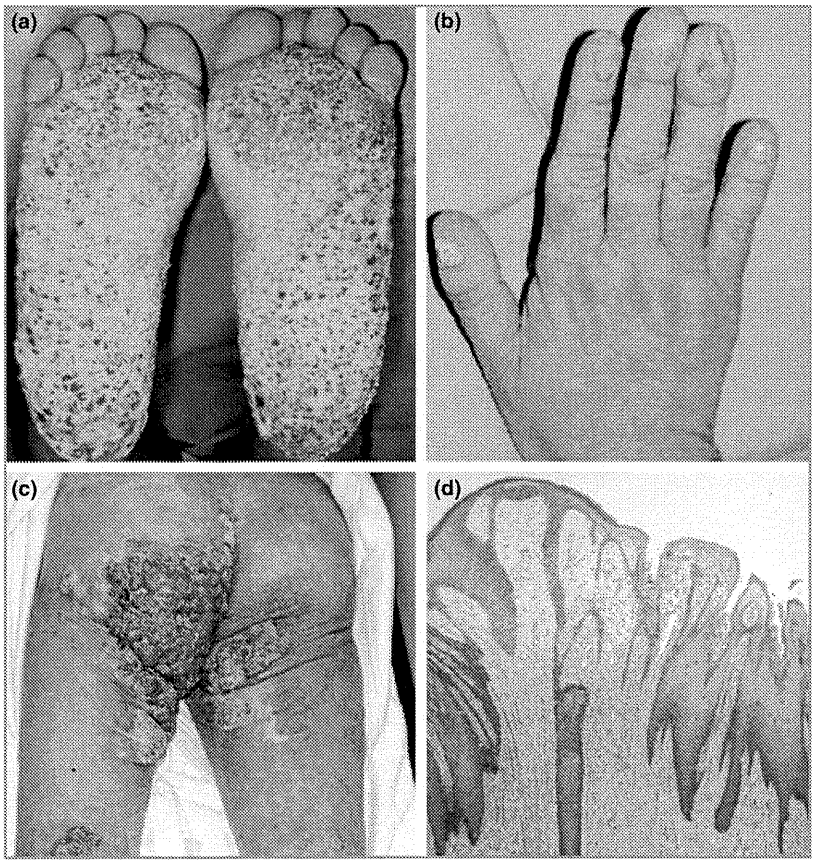

Fig 1. Clinical features of the proband. (a) Numerous erosive papules are coalesced into a hyperkeratotic plaque on the proband's soles. (b) Nail dystrophy is seen in the fingers. (c) A tumour is observed on the left buttock. Scars after skin abrasion are seen on the dorsal aspects of the thigh and on the right buttock. (d) Specimens from the tumour show pseudocarcinomatous hyperplasia of the epidermis. Dilated vessels with monocytic infiltrates are seen in the dermis (haematoxylin and eosin; original magnification × 100).

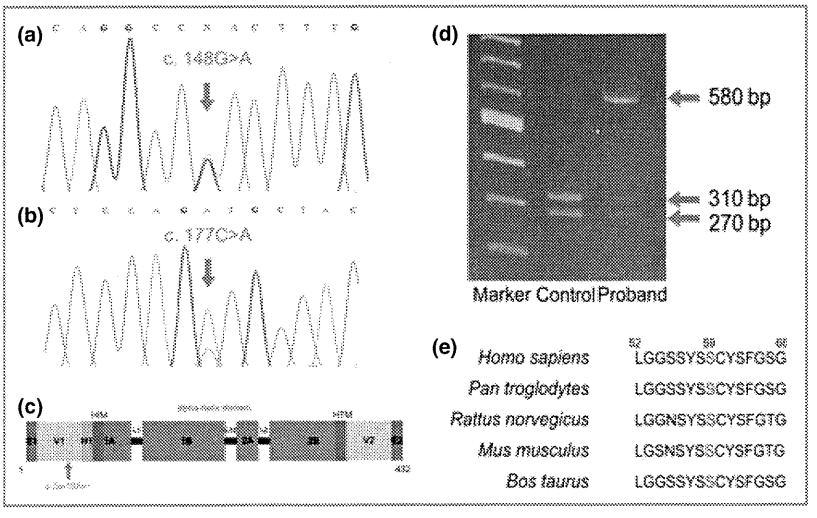

Fig 2. Mutation analysis. (a) The proband was heterozygous for a c.148G>A transition (p.Asp50Asn) mutation in *GJB2* (arrow). (b) c.177C>A (p.Ser59Arg) in *KRT17* was detected in the proband's genomic DNA (arrow). (c) PvuII restriction enzyme digestion of the polymerase chain reaction (PCR) products from genomic DNA of the proband and a normal control. c.177C>A resulted in the loss of a site for PvuII. PvuII restriction enzyme digestion of the PCR products from a normal controls reveals 270- and 310-bp bands. In contrast, 270-, 310- and 580-bp bands were detected in the proband, suggesting that she was heterozygous for c.177C>A. (d) A schematic of the structure of keratin 17. Note that Ser^{59} is located at the V1 region of the keratin molecule (arrow). HIM, helix initiation motif; HTM, helix termination motif. (e) Keratin 17 amino acid sequence alignment shows the level of conservation in diverse species of the amino acid Ser59 (red characters).

GJB2 mutation p.Asp50Asn and may contribute the proband's phenotype. Nevertheless, the limited scope of this study (single case report) does not allow us to determine the clinical significance of p.Ser59Arg in K17, and the influence of other genetic and epigenetic factors cannot be excluded.

*Department of Dermatology, Hokkaido University Graduate School of Medicine, North 15 West 7, Sapporo 060-8638, Japan
†Department of Dermatology, University of Miyazaki Faculty of Medicine, Miyazaki, Japan
‡Department of Dermatology, Nagoya University Graduate School of Medicine, Nagoya, Japan
E-mail: natsuga@med.hokudai.ac.jp

K. NATSUGA*
S. SHINKUMA*
M. KANDA*
Y. SUZUKI*
N. CHOSA†
Y. NARITA†
M. SETOYAMA†
W. NISHIE*
M. AKIYAMA*‡
H. SHIMIZU*

References

1 Mazereeuw-Hautier J, Bitoun E, Chevrant-Breton J *et al.* Keratitis–ichthyosis–deafness syndrome: disease expression and spectrum of connexin 26 (GJB2) mutations in 14 patients. *Br J Dermatol* 2007; **156**:1015–19.
2 Jan AY, Amin S, Ratajczak P *et al.* Genetic heterogeneity of KID syndrome: identification of a Cx30 gene (GJB6) mutation in a patient with KID syndrome and congenital atrichia. *J Invest Dermatol* 2004; **122**:1108–13.
3 Richard G, White TW, Smith LE *et al.* Functional defects of Cx26 resulting from a heterozygous missense mutation in a family with dominant deaf-mutism and palmoplantar keratoderma. *Hum Genet* 1998; **103**:393–9.
4 del Castillo I, Villamar M, Moreno-Pelayo MA *et al.* A deletion involving the connexin 30 gene in nonsyndromic hearing impairment. *N Engl J Med* 2002; **346**:243–9.
5 Kanda M, Natsuga K, Nishie W *et al.* Morphological and genetic analysis of steatocystoma multiplex in an Asian family with pachyonychia congenita type 2 harbouring a KRT17 missense mutation. *Br J Dermatol* 2009; **160**:465–8.
6 Nadeau JH. Modifier genes in mice and humans. *Nat Rev Genet* 2001; **2**:165–74.
7 Szeverenyi I, Cassidy AJ, Chung CW *et al.* The Human Intermediate Filament Database: comprehensive information on a gene family involved in many human diseases. *Hum Mutat* 2008; **29**:351–60.
8 Steinert PM, Mack JW, Korge BP *et al.* Glycine loops in proteins: their occurrence in certain intermediate filament chains, loricrins and single-stranded RNA binding proteins. *Int J Biol Macromol* 1991; **13**:130–9.
9 Terrinoni A, Puddu P, Didona B *et al.* A mutation in the V1 domain of K16 is responsible for unilateral palmoplantar verrucous nevus. *J Invest Dermatol* 2000; **114**:1136–40.
10 Adzhubei IA, Schmidt S, Peshkin L *et al.* A method and server for predicting damaging missense mutations. *Nat Methods* 2010; **7**:248–9.

Funding sources: none.

Conflicts of interest: none declared.

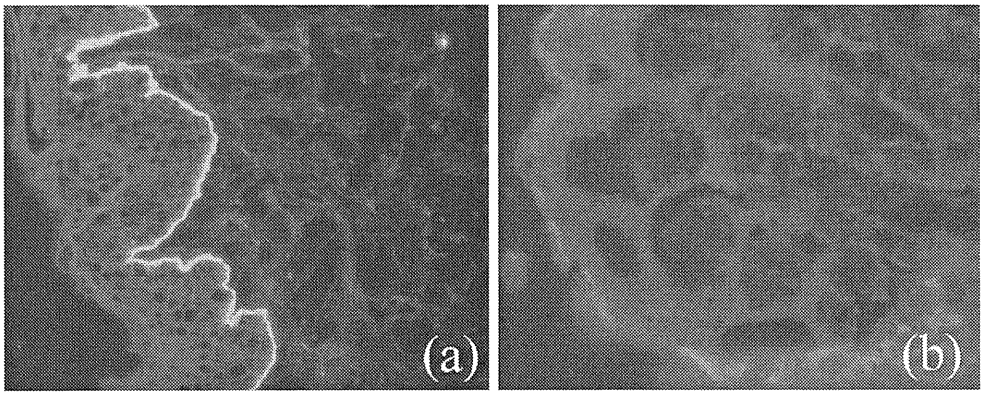

Fig. 2. Indirect immunofluoresence for collagen VII autoantibodies on normal skin (a) and collagen VII deficient skin (b) with serum from EBA patient, 200×.

We agree with the authors that more studies are indicated to determine the use of this test for monitoring disease activity in EBA patients. Similar studies in pemphigus patients with recombinant desmoglein 1 and 3 ELISA's reveal that the sera with identical titers of antibodies by IIF give variable results with ELISA [7]. Unless high titer sera are diluted, saturation of antibody–antigen reactions in ELISA may lead to false low positive ELISA index values to begin with. Such sera may not appear to show a decline in ELISA index values with treatment response [8]. We also have observed, in some pemphigus sera, that even though the IIF titers show a decline, ELISA index values still remain high. Therefore, we may have to use this ELISA with caution to monitor the disease.

References

[1] Saleh MA, Ishii K, Kim YJ, Murakami A, Ishii N, Hashimoto T, et al. Development of NC1 and NC2 domains of Type VII collagen ELISA for the diagnosis and analysis of the time course of epidermolysis bullosa acquisita patients. J Dermatol Sci 2011;62(3):169–75.
[2] Gammon WR, Briggaman RA, Inman III AO, Queen LL, Wheeler CE. Differentiating anti-lamina lucida and anti-sublamina densa anti-BMZ antibodies by indirect immunofluorescence on 1.0 M sodium chloride-separated skin. J Invest Dermatol 1984;82(2):139–44.
[3] Vodegel RM, de Jong MC, Pas HH, Yancey KB, Jonkman MF. Anti-epiligrin cicatricial pemphigoid and epidermolysis bullosa acquisita: differentiation by use of indirect immunofluorescence microscopy. J Am Acad Dermatol 2003;48(4):542–7.
[4] Parker SR, MacKelfresh J. Autoimmune blistering diseases in the elderly. Clin Dermatol 2011;29(1):69–79.
[5] Ishii N, Yoshida M, Hisamatsu Y, Ishida-Yamamoto A, Nakane H, Iizuka H, et al. Epidermolysis bullosa acquisita sera react with distinct epitopes on the NC1 and NC2 domains of type VII collagen: study using immunoblotting of domain-specific recombinant proteins and postembedding immunoelectron microscopy. Br J Dermatol 2004;150(5):843–51.
[6] Ishii N, Yoshida M, Ishida-Yamamoto A, Fritsch A, Elfert S, Bruckner-Tuderman L, et al. Some epidermolysis bullosa acquisita sera react with epitopes within the triple-helical collagenous domain as indicated by immunoelectron microscopy. Br J Dermatol 2009;160(5):1090–3.
[7] Bystryn JC, Akman A, Jiao D. Limitations in enzyme-linked immunosorbent assays for antibodies against desmogleins 1 and 3 in patients with pemphigus. Arch Dermatol 2002;138(9):1252–3.
[8] Cheng SW, Kobayashi M, Kinoshita-Kuroda K, Tanikawa A, Amagai M, Nishikawa T. Monitoring disease activity in pemphigus with enzyme-linked immunosorbent assay using recombinant desmogleins 1 and 3. Br J Dermatol 2002; 147(2):261–5.

E. Eugene Bain[a], Raminder K. Grover[b,*], Richard W. Plunkett[b], Ernst H. Beutner[a,b]

[a]*Department of Dermatology, School of Medicine and Biomedical Sciences, University at Buffalo, State University of New York, Buffalo, NY 14203, USA*;

[b]*Beutner Laboratories and the Department of Microbiology and Immunology, School of Medicine and Biomedical Sciences, University at Buffalo, State University of New York, Buffalo, NY 14214, USA*

*Corresponding author at: 138 Farber Hall, Beutner Laboratories and the Departments of Microbiology and Immunology, School of Medicine and Biomedical Sciences, University at Buffalo, SUNY, Buffalo, NY 14215, USA. Tel.: +1 716 838 0549; fax: +1 716 838 0798
E-mail address: rgrover2@buffalo.edu (R.K. Grover)

27 July 2011

doi:10.1016/j.jdermsci.2011.12.004

Letter to the Editor

CYP4F22 is highly expressed at the site and timing of onset of keratinization during skin development

Keywords:
Ichthyosis;
Keratinization;
Skin barrier

Autosomal recessive congenital ichthyoses (ARCI) include several subtypes: harlequin ichthyosis (HI), lamellar ichthyosis (LI) and congenital ichthyosiform erythroderma (CIE). To date, six causative genes have been identified in ARCI patients: *ABCA12*, *TGM1*, *NIPAL4*, *CYP4F22*, *ALOXE3* and *ALOX12B* [1]. The localization of transglutaminase 1, ABCA12 and 12R-lipoxygenase have been analyzed using samples from patients and model mice [1]. However, as for NIPAL4, CYP4F22, and lipoxygenase-3, neither localization nor function has been fully clarified yet. Herein, we investigate the expression pattern and localization of NIPAL4, CYP4F22 and lipoxygenase-3 in developing human epidermis and primary cultured normal human keratinocytes.

By quantitative reverse transcription (RT)-PCR analysis, at 10 and 14 weeks EGA, mRNA of *NIPAL4*, *CYP4F22* and *ALOXE3* was hardly expressed (Fig. 1A). The *CYP4F22* mRNA expression at 18

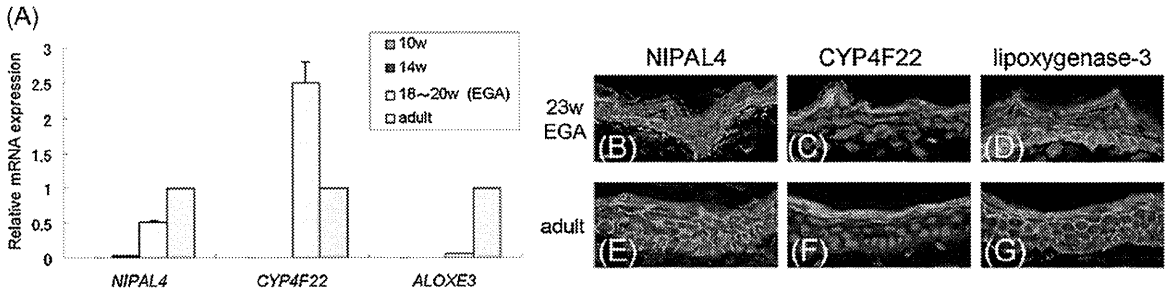

Fig. 1. NIPAL4, CYP4F22 and lipoxygenase-3 expression in developing human skin. (A) mRNA expression in developing human skin. The mRNA expression of *NIPAL4*, *CYP4F22* and *ALOXE3* in fetal human whole skin was studied by quantitative RT-PCR analysis, normalized by *GAPDH* [Applied Biosystems: Hs00398027_m1*, Hs00403446_m1*, Hs00222134_m1*, Hs03929097_ gl*]. At 10 and 14 weeks EGA, *NIPAL4*, *CYP4F22* and *ALOXE3* mRNA are hardly expressed. At 18–20 weeks EGA, the rate of *CYP4F22* mRNA expression is higher than in adult human whole skin ($n = 3$, mean ± SD). (B–G) Immunofluorescence staining of NIPAL4, CYP4F22 and lipoxygenase-3 in developing human skin. Fetal skin samples at 10–23 weeks EGA and adult skin samples were stained for NIPAL4 [Rabbit polyclonal anti-NIPAL4 antibody against a 16-amino acid sequence synthetic peptide (residues 445–461)], CYP4F22 [B01; Abnova, Taipei City, Taiwan], and lipoxygenase-3 [T-14; Santa Cruz Biotechnology, Santa Cruz, CA, U.S.A.] (Supplementary Fig. S1). For the 23 weeks EGA sample and the adult skin, CYP4F22 (C and F) is expressed in the upper layer of the epidermis, mainly in the granular layers. NIPAL4 (B and E) and lipoxygenase-3 (D and G) are expressed at the cell periphery throughout the epidermis. NIPAL4 expression is seen evenly from the basal cell layer to the granular layers, although lipoxygenase-3 expression is slightly stronger towards the granular layers. NIPAL4, CYP4F22 and lipoxygenase-3 green (FITC), nuclear stain, red (PI solution) (original magnification 40×). Data are presented as representative of triplicate experiments.

and 20 weeks EGA was higher than that in adult human skin. At 18 and 20 weeks EGA, *NIPAL4* mRNA expression was approximately half of that in adult skin, and only a tiny amount of *ALOXE3* mRNA was expressed.

We investigated protein localization by immunofluorescence staining (Fig. 1B–G). For the 10 weeks EGA sample, NIPAL4, CYP4F22 and lipoxygenase-3 were not detected. A similar pattern was obtained for the 14 weeks EGA sample. For the 23 weeks EGA sample, CYP4F22 was expressed in the upper layer of epidermis, mainly in the granular layers, and NIPAL4 and lipoxygenase-3 were expressed at the cell periphery in the entire epidermis. Staining patterns of NIPAL4, CYP4F22 and lipoxygenase-3 in the adult skin were similar to those at 23 weeks EGA. Lipoxygenase-3 is usually considered to be a partner with 12R-LOX. 12R-LOX has been visualized at the cell periphery only in the upper epidermis [2]. In our results, lipoxygenase-3 was distributed at the cell periphery in the entire epidermis. Concerning to lipoxygenase-3 in the upper epidermis, lipoxygenase-3 is thought to work with 12R-LOX, although function of lipoxygenase-3 in the lower epidermis is unknown.

In cultured keratinocytes, RT-PCR analysis (Fig. 2A) and immunoblot analysis (Fig. 2B and C) confirmed that mRNA and protein expression of CYP4F22 were increased under the high Ca^{2+} condition (1.2 mmol/L for 48 h). In contrast, there was no significant increase in the mRNA or protein expression of NIPAL4 or ALOXE3 under the high Ca^{2+} condition.

The present study of the adult human epidermis clarified that NIPAL4 and lipoxygenase-3 were expressed at the cell periphery in the entire epidermis of adult human skin. CYP4F22 was expressed in the cytoplasm of keratinocytes in the upper layer of adult human epidermis, mainly in the granular layers. One previous report [3] noted that, inconsistent with our present observations, *NIPAL4* mRNA is highly expressed in the granular layers of the epidermis with *in situ* hybridization analysis. The cause of this discrepancy is unclear, but it might be due to difference in sensitivity between *in situ* hybridization and immunostaining.

We have demonstrated that the mRNAs of *NIPAL4*, *CYP4F22* and *ALOXE3* are not expressed in the early stages of fetal development, at 10 weeks EGA or at 14 weeks EGA. At 18 and 20 weeks EGA, *NIPAL4* mRNA expression was about half that in adult skin, although *ALOXE3* mRNA was only weakly expressed. Among the keratinization-associated genes, the mRNA expression pattern of *NIPAL4* is similar to that of *ABCA12*, and the pattern of *ALOXE3* resembles those of other keratinization-related molecules, such as *TGM1*, *LOR* and *KLK7* [4].

NIPAL4 encodes a putative transmembrane protein of 404 amino acids with a molecular weight of 44 kDa [6]. The NIPAL4 protein is highly expressed in the brain, lung and stomach, and in

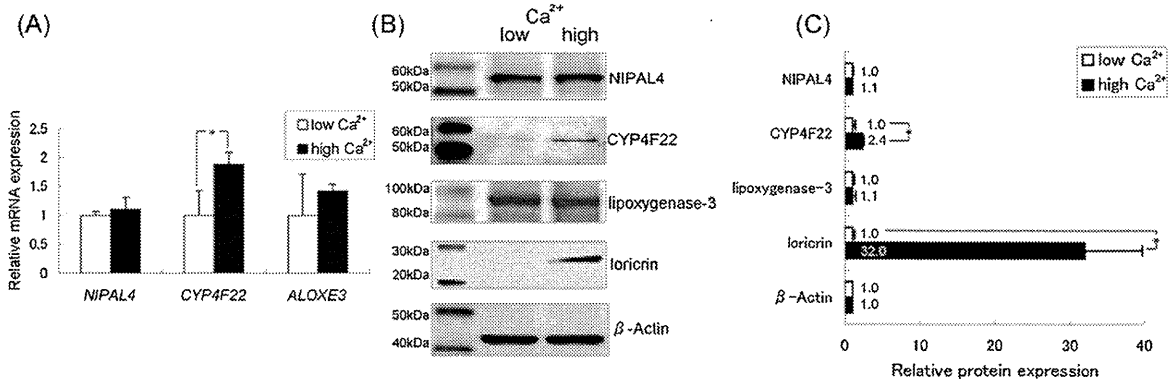

Fig. 2. mRNA and protein expression of NIPAL4, CYP4F22 and ALOXE3 in developing human skin and NHEK. (A) mRNA expression in NHEK. mRNA expression of *CYP4F22* is significantly higher in the NHEK under the high Ca^{2+} condition than in those under the low Ca^{2+} condition. There are no significant differences between the high and low Ca^{2+} conditions in terms of the mRNA expression of *NIPAL4* and *ALOXE3* ($n = 3$, mean ± SD, $^*p < 0.05$). (B) Protein expression assessed by Western blot analysis. The expression of CYP4F22 is higher in the NHEK raised under the high Ca^{2+} condition than in those raised under the low Ca^{2+} condition. However, neither NIPAL4 nor lipoxygenase-3 is increased under high Ca^{2+} condition. Anti-ALOXE3 antibody for immunoblotting: NBP1-32533; Novus Biologicals, LLC, U.S.A. (C) Quantitative analysis by Image J software revealed that the protein expression of CYP4F22 was significantly increased under the high Ca^{2+} condition. Data are presented as representative of triplicate experiments.

leukocytes and keratinocytes. The protein product of the *ALOXE3* gene, lipoxygenase-3, is thought to function as a hydroperoxide isomerase to generate epoxy alcohol [5]. CYP4F22 is a member of the cytochrome P450 family 4, subfamily F. The gene includes 12 coding exons and the cDNA spans 2.6 kb in length. All *CYP4F22* mutations reported to date are predicted to abolish the function of the encoded CYP protein and to compromise the 12(R)-lipoxygenase (hepoxilin) pathway.

Human epidermis contains 15S-lipoxygenase type 1, 12S-lipoxygenase and 12R-lipoxygenase [6]. Skin also contains cytochrome 450, and members of the CYP4 family with unknown epidermal function [3]. 12R-lipoxygenase has attracted great medical interest. 12R-lipoxygenase is expressed only in the epidermis and the tonsils [6,7] and is upregulated in psoriatic lesions [8]. It transforms 20:4n-6 to 12R-hydroperoxyeicosatetraenoic acid (12R-HPETE), which is important for the development of the water permeability barrier function in the epidermis [2]. 12R-LOX and eLOX3 play a crucial role in releasing ω-hydroxyceramide for construction of the corneocyte lipid envelope which is essential for intact skin barrier [9]. O-linoleoyl-ω-hydroxyceramide is oxygenated by the consecutive actions of 12R-LOX and eLOX3 and the products are covalently attached to protein *via* the free ω-hydroxyl of the ceramide, forming the corneocyte lipid envelope [9].

It is hypothesized that CYP4F22 may be linked to the 12R-lipoxygenase and lipoxygenase-3 pathway. Hydroxyeicosatetraenoic acids (HEETs) can be hydrolyzed to triols by epoxide hydrolases, and these products might be substrates of CYP4F members. Thus, it is possible that CYP4F22 might be involved in a downstream step in the 12R-lipoxygenase/lipoxygenase-3 pathway. CYP4F22 could be involved in the oxidation of 8R,11R,12R-HEET. However, from a systemic study of MS/MS spectra of HEETs derived from 12- and 15-HPETE, CYP4F22 did not appear to oxidize 8R,11R,12R-HEET [10]. Nilsson et al. [10] reported that recombinant CYP4F22 catalyzed the omega-3 hydroxylation of 20:4n-6; however, oxygenation of 8R,11R,12R-HEET was not detected. An additional function of CYP4F22 is to synthesize the omega-hydroxy fatty acids in the ceramide [10].

Our study revealed CYP4F22 to be highly expressed at the site and the onset of keratinization during skin development. From this it is speculated that CYP4F22 is involved in the metabolism of lipid substrates that are important to differentiation/keratinization of epidermal keratinocytes, at least during the fetal period. Further studies of the function of CYP4F22 would be needed to elucidate its function in development of the epidermis and keratinocytes.

Acknowledgments

This work was supported in part by Grants-in-Aid from the Ministry of Education, Science, Sports and Culture of Japan (Kiban A 23249058 to M. Akiyama), a grant from the Ministry of Health, Labor and Welfare of Japan (Health and Labor Sciences Research grants; Research on Intractable Diseases: H22-177 to M. Akiyama) and the Health and Labor Sciences Research Grant (Research on Allergic Diseases and Immunology; H21-Meneki- Ippan-003 to H. Shimizu). We thank Sapporo Maternity Women's Hospital (Sapporo, Japan) for providing fetal skin samples.

Appendix A. Supplementary data

Supplementary data associated with this article can be found, in the online version, at doi:10.1016/j.jdermsci.2011.12.006.

References

[1] Akiyama M. Updated molecular genetics and pathogenesis of ichthyoses. Nagoya J Med Sci 2011;73:79–90.
[2] Epp N, Fürstenberger G, Müller K, de Juanes S, Leitges M, Hausser I, et al. 12R-lipoxygenase deficiency disrupts epidermal barrier function. J Cell Biol 2007;177:173–82.
[3] Wajid M, Kurban M, Shimomura Y, Christiano AM. NIPAL4/ichthyin is expressed in the granular layer of human epidermis and mutated in two Pakistani families with autosomal recessive ichthyosis. Dermatology 2010;220:8–14.
[4] Yamanaka Y, Akiyama M, Sugiyama-Nakagiri Y, Sakai K, Goto M, McMillan JR, et al. Expression of keratinocyte lipid transporter ABCA12 in developing and reconstituted human epidermis. Am J Pathol 2007;171:43–52.
[5] Eckl KM, Krieg P, Küster W, Traupe H, André F, Wittstruck N, et al. Mutation spectrum and functional analysis of epidermis-type lipoxygenases in patients with autosomal recessive congenital ichthyosis. Hum Mutat 2005;26:351–61.
[6] Holtzman MJ, Turk J, Pentland A. A regiospecific monooxygenase with novel stereopreference is the major pathway for arachidonic acid oxygenation in isolated epidermal cells. J Clin Invest 1989;84:1446–53.
[7] Boeglin WE, Kim RB, Brash AR. A 12R-lipoxygenase in human skin: mechanistic evidence, molecular cloning, and expression. Proc Natl Acad Sci USA 1998;95:6744–9.
[8] Woollard PM. Stereochemical difference between 12-hydroxy-5,8,10,14-eicosatetraenoic acid in platelets and psoriatic lesions. Biochem Biophys Res Commun 1986;136:169–76.
[9] Zheng Y, Yin H, Boeglin WE, Elias PM, Crumrine D, Beier DR, et al. Lipoxygenases mediate the effect of essential fatty acid in skin barrier formation. A proposed role in releasing omega-hydroxyceramide for construction of the corneocyte lipid envelope. J Biol Chem 2011;286:24046–5.
[10] Nilsson T, Ivanov IV, Oliw EH. LC–MS/MS analysis of epoxyalcohols and epoxides of arachidonic acid and their oxygenation by recombinant CYP4F8 and CYP4F22. Arch Biochem Biophys 2010;494:64–71.

Kaori Sasaki[a], Masashi Akiyama[a,b,*], Teruki Yanagi[a], Kaori Sakai[a], Yuki Miyamura[a], Megumi Sato[a], Hiroshi Shimizu[a]
[a]*Department of Dermatology, Hokkaido University Graduate School of Medicine, Sapporo, Japan*;
[b]*Department of Dermatology, Nagoya University Graduate School of Medicine, Nagoya, Japan*

*Corresponding author at: Department of Dermatology, Nagoya University Graduate School of Medicine, 65 Tsurumai-cho, Showa-ku, Nagoya 466-8550, Japan.
Tel.: +81 52 744 2314
E-mail address: makiyama@med.nagoya-u.ac.jp (M. Akiyama)

1 August 2011

doi:10.1016/j.jdermsci.2011.12.006

5 Quintanilla-Martinez L, Kimura H, Jaffe E. EBV-positive T-cell lymphoproliferative disorders of childhood. In: *WHO Classification of Tumours of Haematopoietic and Lymphoid Tissues* (Swerdlow S, Campo E, Harris N, Jaffe E, Pileri S, Stein H *et al.*, eds), 4th edn. Lyon: IARC Press, 2008; 278–80.
6 Koyama M, Takeshita Y, Sakata A *et al.* Cytotoxic chemotherapy successfully induces durable complete remission in 2 patients with mosquito allergy resulting from Epstein–Barr virus-associated T-/natural killer cell lymphoproliferative disease. *Int J Hematol* 2005; **82**:437–40.
7 Kimura H, Miyake K, Yamauchi Y *et al.* Identification of Epstein–Barr virus (EBV)-infected lymphocyte subtypes by flow cytometric in situ hybridization in EBV-associated lymphoproliferative diseases. *J Infect Dis* 2009; **200**:1078–87.
8 Iwatsuki K, Satoh M, Yamamoto T *et al.* Pathogenic link between hydroa vacciniforme and Epstein–Barr virus-associated hematologic disorders. *Arch Dermatol* 2006; **142**:587–95.

Funding sources: None.

Conflicts of interest: None declared.

Novel adenosine triphosphate (ATP)-binding cassette, subfamily A, member 12 (*ABCA12*) mutations associated with congenital ichthyosiform erythroderma

DOI: 10.1111/j.1365-2133.2011.10516.x

MADAM, Autosomal recessive congenital ichthyosis (ARCI) is a keratinization disorder, characterized by general desquamation. ARCI is a heterogeneous entity, including harlequin ichthyosis (HI, MIM 242500), lamellar ichthyosis type 2 (LI2, MIM 601277) and congenital ichthyosiform erythroderma (CIE, MIM 242100). The reported mutations in CIE include adenosine triphosphate (ATP)-binding cassette, subfamily A, member 12 (*ABCA12*),[1] transglutaminase 1 (*TGM1*),[2] lipoxygenase-3, 12(R)-lipoxygenase,[3] *NIPAL4*[4] and *CYP4F22*.[5] Mutations in *ABCA12* also result in LI2 and HI.[6,7] We report *ABCA12* mutations in four unrelated Japanese patients with CIE and identified five unreported and two recurrent mutations.

Patient 1 is a 3-year-old girl with generalized scales on erythroderma, ectropion, eclabium, severely deformed ears and alopecia (Fig. 1a–c). Her elder sister displayed similar symptoms and died after dehydration and infection. Patient 2 is a 9-year-old girl with generalized scales on an erythrodermic skin, mild ectropion, alopecia of the forehead and mild auricular malformation. Her younger sister died after severe skin symptoms and subsequent complications. Patient 3 is a 4-month-old boy, born as a collodion baby, with systemic whitish scales and generalized erythrodermic skin. There is no family history. Patient 4 is a 3-month-old boy, born as a collodion baby, with generalized whitish scales on a mild erythrodermic skin (Fig. 1d,e). Ectropion, eclabium and auricular malformation were not seen. There is no family history. Pathological findings of all patients revealed hyperkeratosis, mild acanthosis and perivascular lymphocytic infiltration.

We initially examined for *ABCA12* mutation, because *ABCA12* mutations have been found frequently in Japanese patients with CIE. For analysis of the *ABCA12* gene, polymerase chain reaction (PCR) fragments were amplified with 53 primer pairs, as previously reported.[6] We identified five unreported and two recurrent mutations (Table 1). Patient 1 had compound heterozygosity of missense/small deletion mutations [(p.Thr1575Pro)+(c.6031delG)]. Patients 2 and 3 had compound heterozygosity of missense/splice-site mutations [(p.Arg986Trp)+(c.5940–1G>C), (p.Asn1380Ser)+(c.5128+3A>G), respectively]. Patient 4 had compound heterozygosity

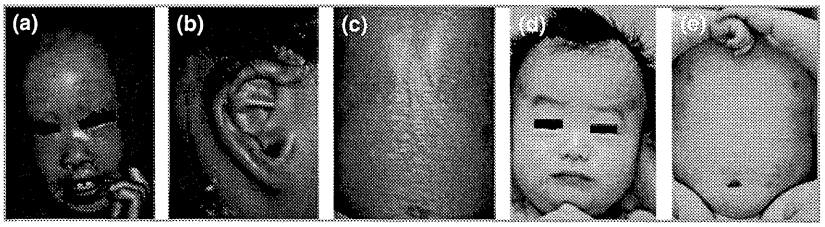

Fig 1. (a–c) Clinical features of patient 1. The whole body was covered with whitish scales on the erythrodermic skin. Ectropion, eclabium and alopecia of the forehead were seen. (d,e) Clinical features of patient 4. Whitish scales and generalized erythrodermic skin were seen.

Table 1 Summary of mutation analysis of *ABCA12* in the present study

Patient	Age, sex	Mutation	Maternal	Paternal
1	3 years, girl	Compound heterozygous	p.Thr1575Pro (c.4723A>C)	c.6031delG
2	9 years, girl	Compound heterozygous	p.Arg986Trp (c.2956C>T)	c.5940–1G>C
3	4 months, boy	Compound heterozygous	p.Asn1380Ser (c.4139A>G)	c.5128+3A>G
4	3 months, boy	Compound heterozygous	p.Thr1575Pro (c.4723A>C)	p.Gly1651Ser (c.4951G>A)

of missense mutations [(p.Thr1575Pro)+(p.Gly1651Ser)]. Each of the parents was a heterozygous carrier. Five mutations (p.Thr1575Pro, c.6031delG, p.Arg986Trp, c.5940–1G>C and c.5128+3A>G) have not been reported previously. Two recurrent mutations (p.Asn1380Ser and p.Gly1651Ser) have been reported previously in LI2.[6] These mutations were not found in 200 normal, unrelated Japanese alleles.

In cDNA from the skin of patient 2, reverse transcriptase-PCR (RT-PCR) across the c.5940–1G>C mutation site showed a single band of 526 bp. Subcloning and direct sequencing

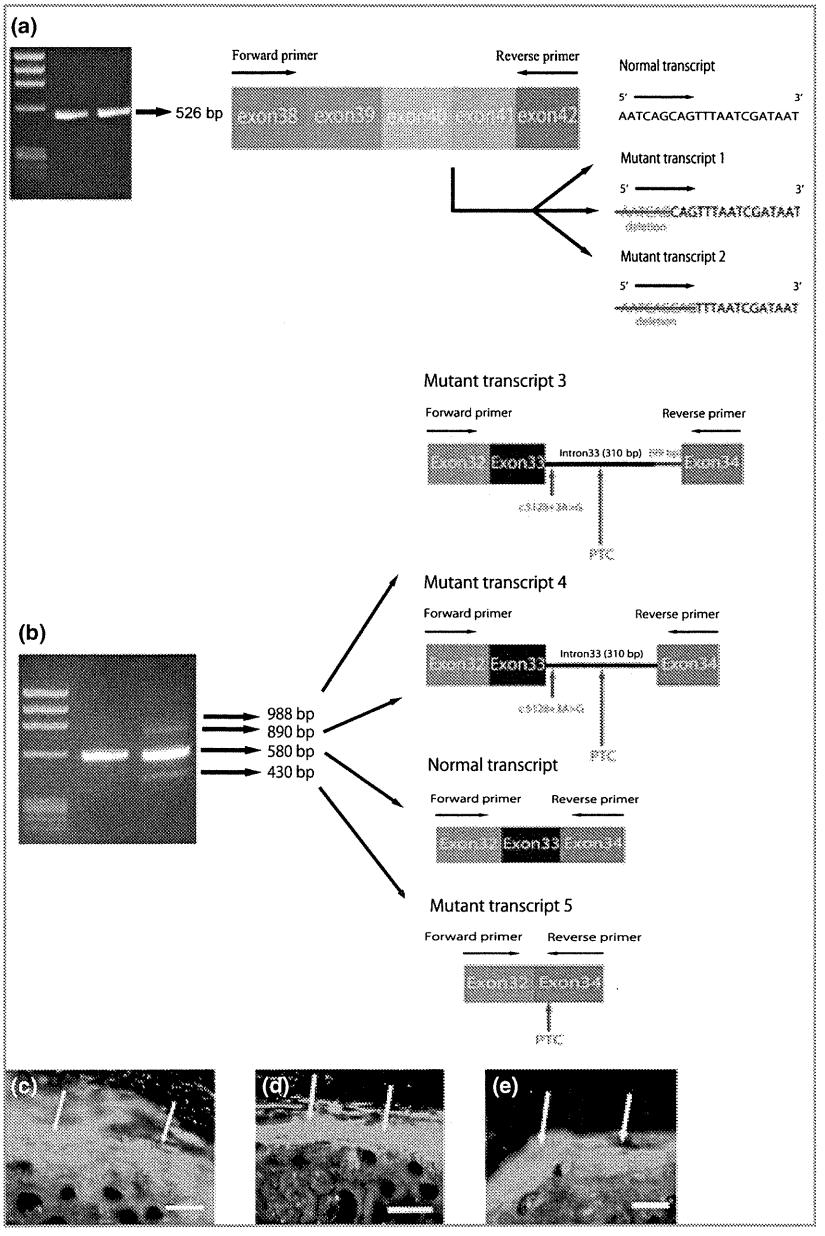

Fig 2. Reverse transcriptase-polymerase chain reaction (RT-PCR) analysis of mRNA fragments around the splice-site mutations and immunofluorescent analysis. (a) In patient 2, RT-PCR, subcloning and direct sequencing through the exon 40–41 boundary revealed two mutant transcripts as well as a normal transcript. Mutant transcript 1 had lost 6-bp nucleotides from exon 41, which resulted in a 2-amino acid deletion (Ile1981_Ser1982del). Mutant transcript 2 had lost 9-bp nucleotides from exon 41, which resulted in a 3-amino acid deletion (Ile1981_Ser1983del). Both mutant transcripts were within-frame deletions. (b) In patient 3, three aberrant mutant transcripts, all of which led to a premature termination codon, were identified by RT-PCR, subcloning and direct sequencing through the exon 33–34 boundary. Mutant transcript 3 was 988 bp in length with the inclusion of 310 bp and another 99 bp of intron 33. Mutant transcript 4 was 890 bp in length with the inclusion of 310 bp of intron 33. Mutant transcript 5 had exon 33 skipping. (c–e) Immunofluorescent labelling of ABCA12 in the skin. (c,d) A dot-like pattern of ABCA12 staining was seen in the cytoplasm of keratinocytes in the upper epidermis in patient 1 (c) and patient 2 (d). (e) In the normal control epidermis, ABCA12 staining was relatively strong in the granular layers and seemed to be dominant at the cell periphery. Bar = 5 μm.

revealed two mutant transcripts with in-frame deletions (Fig. 2a). In cDNA from the skin of patient 3, RT-PCR across the c.5128+3A>G mutation site identified four bands of 988, 890, 580 and 430 bp, with a single 580-bp band in the control sample (Fig. 2b). Subcloning and direct sequencing revealed three aberrant mutant transcripts, all of which led to premature termination codons. Immunofluorescence using anti-ABCA12 antibody revealed a diffuse staining of ABCA12 in the granular layers of control skin (Fig. 2e) and of the non-ABCA12 form (TGM1) from patient CIE (data not shown), while a dot-like staining in the cytoplasm was observed in patients 1 and 2 (Fig. 2c,d).

ABCA12 is a membrane lipid transporter that functions in the lipid transport from the *trans*-Golgi network to lamellar granules.[8] *ABCA12* mutations result in heterogeneity, including LI2, HI and CIE.[1,6,7] LI2 is characterized by generalized scales without serious erythroderma, and caused by either homozygote or compound heterozygote for missense mutations within the first nucleotide-binding folds of *ABCA12*.[6] HI is the severest form of ARCI, characterized by generalized large, plate-like scales with ectropion, eclabium and flattened ears.[7] HI is usually caused by homozygous or compound heterozygous truncation mutations in *ABCA12*.[7] In contrast, CIE with *ABCA12* mutation clinically shows milder manifestations.[1] Thus far, 17 different mutations in *ABCA12* have been reported in 12 cases of CIE. Eleven of 12 cases have at least one missense mutation. Only three of 17 mutations (p.Asn1380Ser, p.Ile1494Thr and p.Arg1514His) were located in the first nucleotide-binding folds. Other mutations were located outside ABCA12 active transporter sites: two nucleotide-binding folds and 12 transmembrane domains. The mutation p.Thr1575Pro was identified in two unrelated patients with different clinical severity. Patient 1 with severer features had a heterozygous truncation mutation (c.6031delG) on another allele, while patient 4, with a milder phenotype, had another heterozygous missense mutation (p.Gly1651Ser). We suggest that the phenotypic variability in these two patients was caused by different mutations.

We identified two *ABCA12* splice-site mutations, which were not reported in CIE: c.5128+3A>G and c.5940–1G>C. RT-PCR analysis across the site of the c.5940–1G>C mutation in patient 2 revealed two mutant transcripts. These findings demonstrate expression of the in-frame shorter transcript lacking two or three amino acids due to this splice-site mutation, which may account for the mild phenotype. In contrast, RT-PCR analysis across the site of the c.5128+3A>G mutation in patient 3 revealed three aberrant mutant transcripts, all of which led to premature termination codons. Therefore, patient 3 had a compound heterozygosity for missense/truncated combinations of mutations.

Using high-throughput sequencing analyses, screening of all ARCI-related genes is currently possible, but the cost is still expensive.[9] Once this is overcome, the elucidation of the pathogenesis of ARCI will greatly progress in the near future.

Acknowledgments

We thank the patients for their participation. We also thank Ms Takako Ishikawa and Ms Ayumi Suzuki for their fine technical assistance, and Ms Akiko Tanaka, Ms Yasuko Nakayama and Ms Hanako Tomita for secretarial work.

Department of Dermatology, Kurume University School of Medicine, and Institute of Cutaneous Cell Biology, 67 Asahimachi, Kurume, Fukuoka 830-0011, Japan — S. FUKUDA, T. HAMADA, N. ISHII, S. SAKAGUCHI

Department of Dermatology, Hokkaido University Graduate School of Medicine, Sapporo, 060-8638, Japan — K. SAKAI*, M. AKIYAMA†, H. SHIMIZU*

†*Department of Dermatology, Nagoya University Graduate School of Medicine, Nagoya, 466-8550, Japan* — K. MASUDA‡, K. IZU§

‡*Department of Dermatology, Kyoto Prefectural University of Medicine Graduate School of Medical Science, Kyoto, 62-8566, Japan* — K. TEYE, D. TSURUTA, T. KARASHIMA

§*Department of Dermatology, Kyushu Kosei-Nenkin Hospital, Kitakyushu, 806-8501, Japan* — T. NAKAMA, S. YASUMOTO

Correspondence: Takashi Hashimoto. — T. HASHIMOTO

E-mail: hashimot@med.kurume-u.ac.jp

References

1 Natsuga K, Akiyama M, Kato N *et al.* Novel ABCA12 mutations identified in two cases of non-bullous congenital ichthyosiform erythroderma associated with multiple skin malignant neoplasia. *J Invest Dermatol* 2007; **127**:2669–73.

2 Laiho E, Ignatius J, Mikkola H *et al.* Transglutaminase 1 mutations in autosomal recessive congenital ichthyosis: private and recurrent mutations in an isolated population. *Am J Hum Genet* 1997; **61**:529–38.

3 Jobard F, Lefèvre C, Karaduman A *et al.* Lipoxygenase-3 (ALOXE3) and 12(R)-lipoxygenase (ALOX12B) are mutated in non-bullous congenital ichthyosiform erythroderma (NCIE) linked to chromosome 17p13.1. *Hum Mol Genet* 2002; **11**:107–13.

4 Lefèvre C, Bouadjar B, Karaduman A *et al.* Mutations in ichthyin a new gene on chromosome 5q33 in a new form of autosomal recessive congenital ichthyosis. *Hum Mol Genet* 2004; **13**:2473–82.

5 Lefèvre C, Bouadjar B, Ferrand V *et al.* Mutations in a new cytochrome P450 gene in lamellar ichthyosis type 3. *Hum Mol Genet* 2006; **15**:767–76.

6 Lefèvre C, Audebert S, Jobard F *et al.* Mutations in the transporter ABCA12 are associated with lamellar ichthyosis type 2. *Hum Mol Genet* 2003; **12**:2369–78.

7 Akiyama M, Sugiyama-Nakagiri Y, Sakai K *et al.* Mutations in ABCA12 in harlequin ichthyosis and functional recovery by corrective gene transfer. *J Clin Invest* 2005; **115**:1777–84.

8 Sakai K, Akiyama M, Sugiyama-Nakagiri Y *et al.* Localization of ABCA12 from Golgi apparatus to lamellar granules in human upper epidermal keratinocytes. *Exp Dermatol* 2007; **16**:920–6.

9 Pastinen T. Genome-wide allele-specific analysis: insights into regulatory variation. *Nat Rev Genet* 2010; **11**:533–8.

Funding sources: This study was supported by Grants-in-Aid for Scientific Research and Strategic Research Basis Formation Supporting Project from the Ministry of Education, Culture, Sports, Science and Technology of Japan, and by Health and Labour Sciences Research Grants and grants for Research on Measures for Intractable Diseases from the Ministry of Health, Labour and Welfare of Japan. The study was also supported by grants from the Uehara Memorial Foundation, the Nakatomi Foundation, the Kaibara

Morikazu Medical Science Promotion Foundation, the Japan Lydia O'Leary Memorial Foundation, the Cosmetology Research Foundation, the Japanese Dermatological Association (Shiseido Award), the Fukuoka Foundation for Sound Health, and Galderma K.K. (Galderma Award).

Conflicts of interest: None declared.

Iatrogenic androgenetic alopecia in a male phenotype 46XX true hermaphrodite

DOI: 10.1111/j.1365-2133.2011.10511.x

MADAM, Androgenetic alopecia (AGA) is a term that describes the androgen-dependent and genetically determined nature of the disease.[1] However, although it is known that androgen replacement therapy can induce AGA, no report has previously been issued regarding the development of iatrogenic AGA in a hermaphrodite undergoing androgen therapy. Herein, we describe a unique case of a castrated male phenotype 46XX true hermaphrodite receiving exogenous androgen supplementation who developed male-type hair loss.

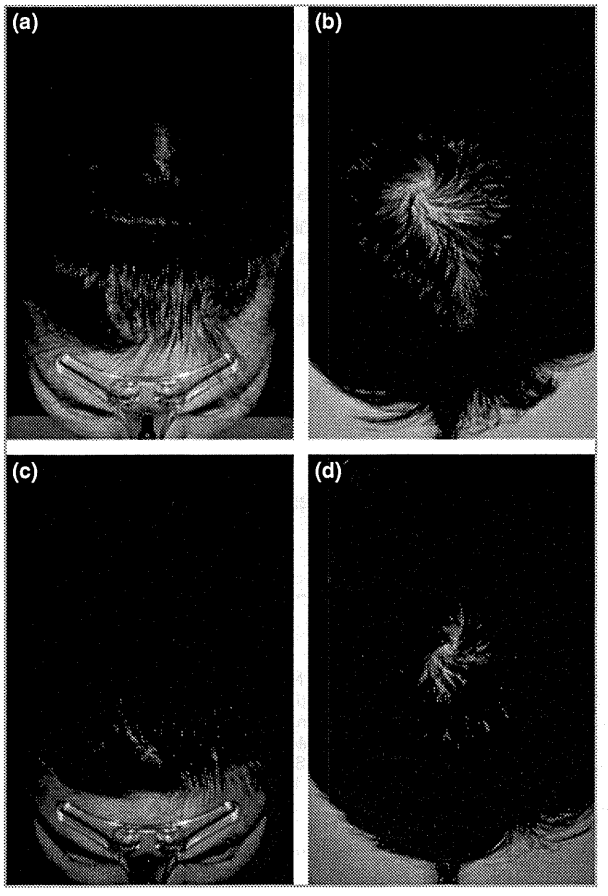

Fig 1. Iatrogenic androgenetic alopecia in a male phenotype 46XX true hermaphrodite showed a great improvement compared with baseline (a, b) after 4 months of finasteride treatment (c, d).

A 21-year-old male phenotype 46XX true hermaphrodite presented with a 3-year history of progressive hair loss. At the age of 16 years he was diagnosed as a 46XX true hermaphrodite with bilateral ovotestis, and subsequently underwent bilateral orchiectomy and testis prosthesis insertion. In addition, he was then given testosterone replacement therapy (testosterone enanthate, Jenasteron®; Jenapharm, Jena, Germany) for surgically induced andropausal status, which halted the development of secondary sexual characteristics. After 3 years of androgen therapy, progressive hair thinning developed on the scalp. Hair examination revealed nonscarring Norwood–Hamilton type III vertex alopecia with frontotemporal recession or BASP classification M1V2 alopecia (Fig. 1a, b).[2] Digital microscopy (Folliscope®; LeadM Corporation, Seoul, Korea) showed miniaturized hair shafts, and hair shaft size variation over the vertex scalp (Fig. 2). Serum testosterone, at the time, was 4·1 ng mL^{-1} (normal 2·7–10·7) and serum dehydroepiandrosterone sulphate was 1845 ng mL^{-1} (normal 800–5600). Under a diagnosis of iatrogenic androgen-induced alopecia, finasteride (1 mg daily) therapy was started. After 4 months of treatment, the hair loss stabilized and scalp hair regrowth was observed, despite the continuance of testosterone replacement therapy (Fig. 1c, d).

True hermaphroditism is an extremely rare disorder, which is defined as the coexistence of testicular and ovarian tissue in the same subject. The most frequent karyotype of true hermaphrodites is 46XX.[3] Gender assignments for hermaphrodites are made according to genetic, gonadal, social and psychologically determined sex, and the requests of patients and their relatives.[4] To be reared as male or female, surgical correction of ambiguous external genitalia, surgical removal of dysgenetic gonads, and sex hormone replacement for the surgically induced andropausal or menopausal state are required. The unwanted dermatological side-effects of testosterone replacement therapy include acne, excessive hair growth and male pattern baldness. As in our case, to be reared

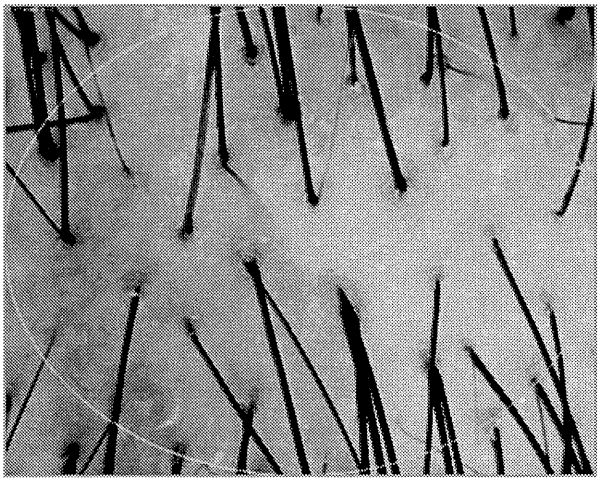

Fig 2. Photomicrograph showing miniaturized hair shafts, and variations in hair shaft size over the vertex scalp (original magnification ×50).

RHEUMATOLOGY

Rheumatology 2012;51:129–133
doi:10.1093/rheumatology/ker333
Advance Access publication 9 November 2011

Concise report

Investigation of prognostic factors for skin sclerosis and lung function in Japanese patients with early systemic sclerosis: a multicentre prospective observational study

Minoru Hasegawa[1], Yoshihide Asano[2], Hirahito Endo[3], Manabu Fujimoto[1], Daisuke Goto[4], Hironobu Ihn[5], Katsumi Inoue[6], Osamu Ishikawa[7], Yasushi Kawaguchi[8], Masataka Kuwana[9], Yoshinao Muro[10], Fumihide Ogawa[11], Tetsuo Sasaki[12], Hiroki Takahashi[13], Sumiaki Tanaka[14], Kazuhiko Takehara[1] and Shinichi Sato[2]

Abstract

Objective. To clarify the clinical course of SSc in Japanese patients with early-onset disease. It is well known that ethnic variations exist in the clinical features and severity of SSc. However, neither the clinical course nor prognostic factors have been thoroughly investigated in the Japanese population.

Methods. Ninety-three Japanese patients of early-onset SSc (disease duration: <3 years) with diffuse skin sclerosis and/or interstitial lung disease were registered in a multi-centre observational study. All patients had a physical examination with laboratory tests at their first visit and at each of the three subsequent years. Factors that could predict the severity of skin sclerosis and lung involvement were examined statistically by multiple regression analysis.

Results. Two patients died from SSc-related myocardial involvement and four patients died from other complications during the 3-year study. Among various clinical data assessed, the initial modified Rodnan total skin thickness score (MRSS) and maximal oral aperture were associated positively and negatively with MRSS at Year 3, respectively. Additionally, initial ESR tended to be associated with final MRSS. Pulmonary vital capacity (VC) in the third year was significantly associated with initial %VC. Furthermore, patients with anti-topo I antibody tended to show reduced %VC at Year 3.

Conclusions. Several possible prognostic factors for skin sclerosis and lung function were detected in Japanese patients with early SSc. Further longitudinal studies of larger populations will be needed to confirm these findings.

Key words: systemic sclerosis, scleroderma, prognostic factor, skin sclerosis, interstitial lung diseases, treatment

[1]Department of Dermatology, Kanazawa University Graduate School of Medical Science, Kanazawa, [2]Department of Dermatology, Faculty of Medicine, University of Tokyo, Tokyo, [3]Department of Internal Medicine (Omori), Toho University School of Medicine, Tokyo, [4]Department of Rheumatology, Graduate School of Comprehensive Human Sciences, University of Tsukuba, Tsukuba, [5]Department of Dermatology and Plastic Surgery, Faculty of Life Sciences, Kumamoto University, Kumamoto, [6]Division of Rehabilitation Science, Kanazawa University Graduate School of Medical Science, Kanazawa, [7]Department of Dermatology, Gunma University Graduate School of Medicine, Maebashi, [8]Institute of Rheumatology, Tokyo Women's Medical University, [9]Division of Rheumatology, Department of Internal Medicine, Keio University School of Medicine, Tokyo, [10]Department of Dermatology, Nagoya University Graduate School of Medicine, Nagoya, [11]Department of Dermatology, Nagasaki University Graduate School of Biomedical Science, Nagasaki, [12]Department of Dermatology, Atami Hospital, International University of Health and Welfare, Atami, [13]First Department of Internal Medicine, Sapporo Medical University School of Medicine, Sapporo and [14]Department of Rheumatology and Infectious Diseases, Kitasato University School of Medicine, Sagamihara, Japan.

Submitted 12 April 2011; revised version accepted 25 August 2011.

Correspondence to: Minoru Hasegawa, Department of Dermatology, Kanazawa University Graduate School of Medical Science, 13-1 Takaramachi, Kanazawa, Ishikawa 920-8641, Japan.
E-mail: minoruha@derma.m.kanazawa-u.ac.jp

Introduction

SSc is a CTD characterized by tissue fibrosis in the skin and internal organs. Interstitial lung diseases (ILDs) develop in more than half of SSc patients and are one of the major SSc-related causes of death [1, 2]. The natural course of skin sclerosis and internal organ involvement and identification of prognostic factors have been extensively reported in Europe and the USA [3–6]. However, there are some racial differences in the clinical and laboratory features of SSc [7]. For example, the severity of skin sclerosis is modest in Japanese patients [8]. Furthermore, pulmonary arterial hypertension and renal crisis are rare in Japanese SSc patients [9]. Furthermore, racial differences are found in the distribution of SSc-related serum ANAs [10]. The frequency of anti-RNA polymerases antibody (Ab) is lower in the Japanese population than in US or European patient populations [9]. However, there have been no multiple-centre prospective studies concerning the clinical features of SSc in Japanese individuals.

In most patients, severe organ involvement occurs within the first 3 years of disease and skin sclerosis seldom progresses after 5 or 6 years [3, 11]. Therefore, predicting disease progression is particularly important for SSc patients at their first visit. In the present study, we aimed to determine if any initial clinical or laboratory features were associated with subsequent disease severity in Japanese SSc patients with a short disease duration of <3 years.

Materials and methods

Patients

Patients were grouped according to the degree of skin involvement, based on the classification system proposed by LeRoy *et al.* (dcSSc *vs* lcSSc) [12]. In this study, 93 Japanese patients with early SSc (disease duration: <3 years) who had dcSSc or ILD were registered at 12 major scleroderma centres in Japan (Atami Hospital, International University of Health and Welfare; Gunma University Hospital; Kanazawa University Hospital; Keio University Hospital; Kitasato University Hospital; Kumamoto University Hospital; Nagasaki University Hospital; Nagoya University Hospital; Sapporo Medical University Hospital; Tokyo University Hospital; Tokyo Women's Medical University Hospital; Tsukuba University Hospital).

Among these patients, two died from SSc-related myocardial involvement and four died from complications (ANCA-associated vasculitis, sepsis, thrombotic thrombocytopenic purpura and uterine cancer, respectively) during the 3-year study. Therefore, 87 patients (49 patients had dcSSc with ILD, 27 patients had dcSSc without ILD and 11 patients had lcSSc with ILD) were followed for 3 years. Sixty-four were females and 23 were males; the median (range) age was 50 (3–74) years. All patients fulfilled the criteria for SSc proposed by the ACR [13]. The median (range) disease duration (the period from the development of any symptoms excluding RP to our first assessment) of patients was 20 (1–35) months. With respect to ANA, 56 patients were positive for anti-topo I Ab and 7 patients were positive for ACA. Medical ethics committee of Kanazawa University approved the study. In addition, this study was approved by the ethics committees of International University of Health and Welfare, Gunma University, Keio University, Kitasato University, Kumamoto University, Nagasaki University, Nagoya University, Sapporo Medical University, Tokyo University, Tokyo Women's Medical University and Tsukuba University. Informed consent was obtained from all patients.

Clinical assessments

Patients had a physical examination and laboratory tests performed at their first visit and at each subsequent year for 3 years. The degree of skin involvement was determined according to the modified Rodnan total skin thickness score (MRSS), as described elsewhere [14]. Organ system involvement was defined as described previously [15] with some modifications: ILD = bibasilar interstitial fibrosis or ground-glass shadow on high-resolution CT (HRCT); pulmonary arterial hypertension (PAH) = clinical evidence of pulmonary hypertension and elevated right ventricular systolic pressure (>45 mmHg) documented by echocardiography in the absence of severe pulmonary interstitial fibrosis; oesophagus = apparent dysphasia, reflux symptoms or hypomotility shown by barium radiography; heart = pericarditis, congestive heart failure or arrhythmias requiring treatment; kidney = malignant hypertension and rapidly progressive renal failure unexplained by certain diseases other than SSc; joint = inflammatory polyarthralgias or arthritis; and muscle = proximal muscle weakness and elevated serum creatine kinase. An HAQ modified for Japanese patients [16], digital ulcer, pitting scar, maximal oral aperture (the maximum vertical length of opened mouth) and skin pigmentation/depigmentation were also evaluated. ESR and pulmonary function, including vital capacity (VC) and diffusion capacity for carbon monoxide (DL_{CO}) were also tested.

Statistical analysis

JMP Statistically Discovery Software (SAS institute, Cary, NC, USA) was used for analysis. Potential prognostic factors for the severity of skin sclerosis and lung function were statistically examined by multiple regression analysis. A $P < 0.05$ was considered to be statistically significant. All values are expressed as the median (range).

Results

The clinical course of SSc in Japanese patients

To provide a comprehensive evaluation of the clinical features of SSc in Japanese patients, we analysed clinical data as well as laboratory test results from 87 patients with short disease duration (Table 1). To assess the degree of skin involvement in patients, MRSS values were calculated; VC and DL_{CO} percentages were used to assess lung involvement. For the patient population as a whole, the median (range) MRSS decreased from 17 (2–42) to 12 (0–41) during the first year. The median (range) MRSS

was 12 (0–41) at the end of Year 2 and 10 (0–47) at the end Year 3. Median (range) values for %VC did not significantly change during the 3-year evaluation period: 95 (49–144) at first visit, 93 (26–137) at the end of the first year, 95 (49–144) at the end of the second year and 92 (51–137) at the end of the third year. Similarly, median values for % DL_{CO} did not significantly change during the 3 years.

The frequency of patients with ILD or PAH was stable during the evaluation period. Similarly, the number of patients with oesophageal or joint involvement, pitting scar or skin pigmentation/depigmentation did not vary significantly over time. The value of HAQ and maximal oral aperture did not significantly change during the course. The median (range) value of ESR was 18 (2–95) mm/h at the first visit, then it reduced to 16 (2–84), 13 (1–63) and 12 (0.5–122) mm/h, during the subsequent 3 years. Oral prednisolone (~20 mg/day) use was common, with 56 patients starting to take this drug after the first visit and 70 patients having taken it by the end of Year 3. Two patients developed renal crisis during the course of the study (data not shown). Patients with digital ulcer or heart or muscle involvement were rare during the course (fewer than 10 patients, data not shown).

Prognostic factors of the progress of skin sclerosis

Next, we evaluated clinical or laboratory factors presenting at first visit that could predict the severity of skin sclerosis of 3 years later. Investigated factors were as follows: age, gender, disease duration, anti-topo I Ab, ACA, MRSS at the first visit, %VC, $\%DL_{CO}$, existence of each organ involvement (ILD, PAH, oesophagus, joint), pitting scar, skin pigmentation/depigmentation, HAQ, maximal oral aperture, ESR, CS treatment and cyclophosphamide treatment. Cases that have any missing data were excluded and thereby 80 patients were analysed. We performed multiple regression using stepwise way that specified the α-level for either adding or removing a regression as 0.20 (Table 2). As a result, the multiple regression equation predicting MRSS at the third year = $17.11 + 0.35 \times$ MRSS at the first visit + $-0.26 \times$ maximal oral aperture + $0.042 \times$ ESR ($R^2 = 0.63$, $P < 0.0001$). Thus, MRSS at the third year was significantly associated with MRSS at first visit ($P < 0.001$) and was negatively associated with initial maximal oral aperture at first visit ($P < 0.01$). Additionally, initial ESR tended to be associated with final MRSS ($P = 0.17$).

Prognostic factors of lung function

We similarly assessed the prognostic factors of impaired lung function to estimate ILD severity. Here, we used %VC as representative markers of lung function. Cases that have any missing data including %VC at the third year were excluded and thereby 58 patients were analysed. We performed multiple regression in a stepped manner that specified the α-level for either adding or removing a regression as 0.20 (Table 3). As a result, the multiple regression equation predicting %VC at the third

TABLE 2 Factors predicting MRSS at the third year determined by multiple regression analysis

	Estimate	Standard error	*P*-value
Intercept	17.11	4.88	<0.01
MRSS at the first visit	0.35	0.089	<0.001
Maximal oral aperture	−0.26	0.075	<0.01
ESR	0.042	0.043	0.17

The multiple regression equations predicting MRSS at the third year are as follows; MRSS at the third year = $17.11 + 0.35 \times$ MRSS at the first visit + $-0.26 \times$ maximal oral aperture + $0.042 \times$ ESR. R^2 (determination coefficient) = 0.63; Root mean square error = 4.73; $P < 0.0001$.

TABLE 1 The course of clinical and laboratory features in patients with SSc

	First visit	Year 1	Year 2	Year 3
MRSS	17 (2–42); $n = 87$	12 (0–41); $n = 84$	12 (0–41); $n = 84$	10 (0–47); $n = 87$
%VC	95 (49–144); $n = 70$	93 (26–137); $n = 55$	95 (49–144); $n = 57$	92 (51–137); $n = 60$
$\%DL_{CO}$	70 (11–113); $n = 70$	68 (10–105); $n = 55$	69 (11–96); $n = 57$	68 (10–120); $n = 60$
ILD	54 (62); $n = 87$	47 (64); $n = 73$	47 (64); $n = 73$	46 (63); $n = 73$
PAH	9 (10); $n = 87$	9 (12); $n = 76$	8 (11); $n = 72$	11 (13); $n = 84$
Oesophagus	33 (37); $n = 87$	26 (34); $n = 77$	35 (48); $n = 73$	34 (40); $n = 85$
Joint	20 (23); $n = 86$	14 (18); $n = 77$	9 (12); $n = 73$	17 (20); $n = 84$
Pitting scar	27 (33); $n = 87$	29 (38); $n = 76$	35 (48); $n = 73$	33 (38); $n = 86$
Pigmentation/depigmentation	54 (62); $n = 87$	49 (64); $n = 77$	41 (57); $n = 72$	50 (60); $n = 84$
HAQ	0.08 (0–2); $n = 83$	0.125 (0–1.75); $n = 74$	0.25 (0–2.5); $n = 73$	0.125 (0–2.25); $n = 83$
Maximal oral aperture	45 (18–70); $n = 87$	45 (28–65); $n = 75$	46 (25–67); $n = 72$	45 (10–67); $n = 83$
ESR	18 (2–95); $n = 80$	16 (2–84); $n = 61$	13 (1–63); $n = 52$	12 (0.5–122); $n = 57$
CS	56 (64); $n = 87$	61 (82); $n = 74$	64 (86); $n = 74$	70 (80); $n = 87$
Cyclophosphamide	11 (13); $n = 87$	14 (19); $n = 75$	8 (12); $n = 68$	9 (10); $n = 87$

Values are represented as median (range) or as number of positive cases with percentage within parentheses, in total patients in whom those data are available.

TABLE 3 Factors predicting %VC at the third year determined by multiple regression analysis

	Estimate	Standard error	*P*-value
Intercept	10.94	8.54	0.20
%VC at the first visit	0.85	0.09	<0.0001
Anti-topo I Ab (+)	2.32	1.64	0.19

The multiple regression equations predicting %VC at the third year are as follows: %VC at the third year = 10.94 + 0.85 × %VC at the first visit + anti-topo I Ab ('+' → −2.32, '−' → 2.32). $R^2 = 0.70$; Root mean square error = 12.00; $P < 0.0001$.

year = 10.94 + 0.85 × %VC at the first visit + anti-topo I Ab ('+' → −2.32, '−' → 2.32) ($R^2 = 0.70$, $P < 0.0001$). Thus, %VC at the third year was significantly associated with the value of %VC at first visit ($P < 0.0001$). In addition, %VC at the third year tended to be lower in patients with anti-topoisomerase I Ab ($P = 0.19$).

Discussion

To our knowledge, this study is the first multiple-centre, longitudinal prospective study to investigate the clinical course of Japanese patients. For this study, 87 patients with early-onset SSc (<3 years) were followed over 3 years. Median MRSS was reduced 5 points during the first year, and continued to decrease through the third year. This trend was similar to that identified in our previous, single-centre prospective observational study of Japanese SSc patients [17]. Although the reason for the prominent first-year reduction in MRSS in our current study is unknown, our previous single-centre study [17] indicated that the dose of oral CS was related to the decrease of MRSS. However, in this multi-centre observational study we could not perform a similar analysis of prednisolone dose in patients at each centre. In addition, other therapies including cyclophosphamide were also used in a part of patients in our observational study. Previous large studies demonstrated that MRSS naturally reduced during the disease course and time was a significant predictor of MRSS [3–6]. Therefore, the effect of CS therapy for MRSS remains unclear from our data. Since it has been suggested that CS therapy can induce renal crisis, high doses of CSs have not been recommended for the treatment of SSc [18]. However, renal crisis is not as common in Japanese patients [9], and only two patients (one had been taking low-dose CS, whereas the other had not) developed renal crisis during the course of our study.

The main aim of this study was to define the prognostic factors of skin sclerosis and ILD. The multiple regression equation was defined to predict the MRSS at the third year among multiple factors presenting at the first visit. MRSS at the first visit was significantly correlated with MRSS at the third year in all patients. Maximal oral aperture was correlated inversely with MRSS in the third year. Thus, the current skin sclerosis likely reflects the extent of skin sclerosis of 3 years later independent of other organ's involvement or treatment. Additionally, ESR tended to be associated with final MRSS. The presence of autoantibodies such as anti-topo I Ab and ACA was not shown to have value as a prognostic indicator of MRSS. However, this may be due to population bias in our study, since most patients were positive for anti-topo I Ab and negative for ACA.

The current study revealed that %VC and $\%DL_{CO}$ remained nearly constant or slightly reduced during the 3-year period. Since patients with progressive ILD received immunosuppressive treatment, including cyclophosphamide therapy in the participating facilities, this may have affected the stabilization of lung function in our cases. The frequency of ILD detected by HRCT was not increased during the course of the study, indicating ILD is usually detected early in the disease course and rarely develops later. In consistent with generally stable course of %VC, %VC at their first visit highly associated with the %VC at the third year in all patients with or without treatment. Patients with anti-topo I Ab tended to show reduced %VC at the third year. Although these findings are not surprising, we first confirmed them in Japanese patients.

Our study has some limitations. The population is not large and the follow-up period is not long. This is an observational study and therefore the treatment is heterogeneous. In addition, other parameters including CRP could not be analysed due to the lack of data. We should also include disease activity variables [19] and disease severity scale [20] in our future study. Further longitudinal studies in a larger population will be needed to clarify the natural course and prognostic factors in Japanese SSc patients.

Rheumatology key messages

- Initial ESR tended to be associated with skin score at Year 3 in Japanese scleroderma patients.
- Japanese scleroderma patients with anti-topo I Ab tended to show reduced %VC at the third year.

Acknowledgements

The manuscript has not been previously published nor has it been submitted simultaneously for publication elsewhere. We are grateful to all the physicians who have contributed in assembling the data at each facility. We also thank Tomoko Hayashi and Yuko Yamada for their assistance in registering data.

Funding: This work was supported by funds for research on intractable diseases from the Ministry of Health, Labor, and Welfare of Japan.

Disclosure statement: The authors have declared no conflicts of interest.

References

1 Silver RM. Clinical problems: the lungs. Rheum Dis Clin Nor Am 1996;22:825–40.

2 Steen VD, Conte C, Owens GR, Medsger TA. Severe restrictive lung disease in systemic sclerosis. Arthritis Rheum 1994;37:1283–9.

3 Steen VD, Medsger TA Jr. Severe organ involvement in systemic sclerosis with diffuse scleroderma. Arthritis Rheum 2000;43:2437–44.

4 Tyndall AJ, Bannert B, Vonk M *et al*. Causes and risk factors for death in systemic sclerosis: a study from the EULAR Scleroderma Trials and Research (EUSTAR) database. Ann Rheum Dis 2010;69:1809–15.

5 Walker UA, Tyndall A, Czirjak L *et al*. Clinical risk assessment of organ manifestations in systemic sclerosis: a report from the EULAR Scleroderma Trials And Research group database. Ann Rheum Dis 2007;66:754–63.

6 Amjadi S, Maranian P, Furst DE *et al*. Course of the modified Rodnan skin thickness score in systemic sclerosis clinical trials: analysis of three large multicenter, double-blind, randomized controlled trials. Arthritis Rheum 2009;60:2490–8.

7 Laing TJ, Gillespie BW, Toth MB *et al*. Racial differences in scleroderma among women in Michigan. Arthritis Rheum 1997;40:734–42.

8 Nishioka K, Katayama I, Kondo H *et al*. Epidemiological analysis of prognosis of 496 Japanese patients with progressive systemic sclerosis (SSc). Scleroderma Research Committee Japan. J Dermatol 1996;23:677–82.

9 Hamaguchi Y, Hasegawa M, Fujimoto M *et al*. The clinical relevance of serum antinuclear antibodies in Japanese patients with systemic sclerosis. Br J Dermatol 2008;158:487–95.

10 Kuwana M, Okano Y, Kaburaki J *et al*. Racial differences in the distribution of systemic sclerosis-related serum antinuclear antibodies. Arthritis Rheum 1994;37:902–6.

11 Medsger TA Jr. Classification, purpose. In: Clements PJ, Furst DE, eds. Systemic Sclerosis. Philadelphia: Williams & Wilkins, 2004:17–28.

12 LeRoy EC, Krieg T, Black C *et al*. Scleroderma (systemic sclerosis): classification, subsets, and pathogenesis. J Rheumatol 1988;15:202–5.

13 Committee SfSCotARADaTC. Preliminary criteria for the classification of systemic sclerosis (scleroderma). Arthritis Rheum 1980;23:581–90.

14 Clements P, Lachenbrush P, Seibold J *et al*. Inter and intraobserver variability of total skin thickness score (modified Rodnan TSS) in systemic sclerosis. J Rheumatol 1995;22:1281–5.

15 Steen VD, Powell DL, Medsger TAJ. Clinical correlations and prognosis based on serum autoantibodies in patients with systemic sclerosis. Arthritis Rheum 1988;31:196–203.

16 Kuwana M, Sato S, Kikuchi K *et al*. Evaluation of functional disability using the health assessment questionnaire in Japanese patients with systemic sclerosis. J Rheumatol 2003;30:1253–8.

17 Hasegawa M, Fujimoto M, Matsushita T. Serum chemokine and cytokine levels as indicators of disease activity in patients with systemic sclerosis. Clin Rheumatol 2011;30:231–7.

18 Steen VD, Medsger TA Jr, Osial TA Jr. Factors predicting development of renal involvement in progressive systemic sclerosis. Am J Med 1984;76:779–86.

19 Valentini G, Della Rossa A, Bombardieri S *et al*. European multicentre study to define disease activity criteria for systemic sclerosis. II. Identification of disease activity variables and development of preliminary activity indexes. Ann Rheum Dis 2001;60:592–8.

20 Medsger TA Jr, Silman AJ, Steen VD *et al*. A disease severity scale for systemic sclerosis: development and testing. J Rheumatol 1999;26:2159–67.

observations. First, cutaneous mosaicism has been demonstrated only in dermal fibroblasts or adnexal keratinocytes,[9] both cell types following different embryologic paths from that of melanocytes and both giving rise to nevi which always follow Blaschko's lines (exception: Becker's nevus). Second, melanocytic nevi, in which nevus cells most likely carry the genetic defect, never follow Blaschko's lines, the only exception seemingly being the recently framed "nevus lentiginosus linearis".[10] Thus, I suggest that the relative non-specificity of the syndromic associations of mosaic hypomelanosis and hypermelanosis (excluding McCune–Albright syndrome) might rely on the fact that melanocytes are just "innocent bystanders" of mosaic states affecting other cells and tissues.

Daniele TORCHIA
University of Florence, Florence, Italy

REFERENCES

1 Cabrera HN, Della Giovanna P, Hermida MD. Syndromic nevoid hypermelanosis: description of seven cases with a 10-year follow up. *J Dermatol* 2011; **38**: 125–130.
2 Taibjee SM, Bennett DC, Moss C. Abnormal pigmentation in hypomelanosis of Ito and pigmentary mosaicism: the role of pigmentary genes. *Br J Dermatol* 2004; **151**: 269–282.
3 Kalter DC, Griffiths WA, Atherton DJ. Linear and whorled nevoid hypermelanosis. *J Am Acad Dermatol* 1988; **19**: 1037–1044.
4 Delaporte E, Janin A, Blondel V *et al.* Linear and whorled nevoid hypermelanosis versus incontinentia pigmenti: is pigmentary incontinence really a distinctive feature? *Dermatology* 1996; **192**: 70–72.
5 Hassab-El-Naby HM, Alsaleh QA, Fathallah MA. Linear and whorled nevoid hypermelanosis: report of a case associated with cerebral palsy. *Pediatr Dermatol* 1996; **13**: 148–150.
6 Choi JC, Yang JH, Lee UH, Park HS, Chun DK. Progressive cribriform and zosteriform hyperpigmentation – the late onset linear and whorled nevoid hypermelanosis. *J Eur Acad Dermatol Venereol* 2005; **19**: 638–639.
7 Nehal KS, PeBenito R, Orlow SJ. Analysis of 54 cases of hypopigmentation and hyperpigmentation along the lines of Blaschko. *Arch Dermatol* 1996; **132**: 1167–1170.
8 Gilmore SJ. Patterns in naevoid skin disease: development, disease and modelling. *Exp Dermatol* 2010; **19**: 240–245.
9 Kosaki R, Naito Y, Torii C, Takahashi T, Nakajima T, Kosaki K. Split hand foot malformation with whorl-like pigmentary pattern: phenotypic expression of somatic mosaicism for the p63 mutation. *Am J Med Genet A* 2008; **146A**: 2574–2577.
10 Happle R, Metze D, Vera Casaño A. Naevus lentiginosus linearis: a distinct skin disorder. *Acta Derm Venereol* 2010; **90**: 210–211.

Yellow nail syndrome: Nail change reflects disease severity

Dear Editor,

The triad of yellow nail syndrome (YNS) includes nail yellowing and thickening, lymphedema, and respiratory manifestations.[1] Although the pathogenesis of YNS is unknown, acquired lymphatic dysfunction and microvasculopathy with protein leakage have been thought to be the predominant mechanisms underlying the clinical manifestations.[1,2] YNS has been described in association with malignancies,[3,4] immunodeficiencies[4] and connective tissue diseases.[5] Herein, we report a case of YNS, in which the first manifestation was nail changes alone, then lymphedema and pleural effusion became prominent.

A 71-year-old man was referred to our department with a 5-year history of yellow discoloration of the fingernails and toenails. For 10 years, he had suffered recurrent episodes of chronic sinusitis and pneumonitis. From 3.5 years before his visit, general malaise, dry cough, exertional dyspnea and edema of both legs had presented. Edema of both legs had been improving due to the use of a diuretic. However, the nail changes remained.

When he visited our department, the fingernails and toenails all showed yellowish discoloration, slow growth, absent lunulae, increased curvature and thickening (Fig. 1). Fungal infection was ruled out by KOH examination of the nails. Neither fungus nor bacterium was cultured in the samples taken from the nails.

X-ray and computed tomography of the chest showed bilateral pleural effusions, predominantly in the right lung (Fig. 2).

Thoracentesis revealed light yellow fluid and exudative pleural effusion. No malignant cells were found. Culture of pleural fluid did not identify any bacterial infection. The common causes of transudates (cardiac failure, hepatic cirrhosis, nephropathy) and exudates (lymphoma, metastatic disease, connective tissue disease,

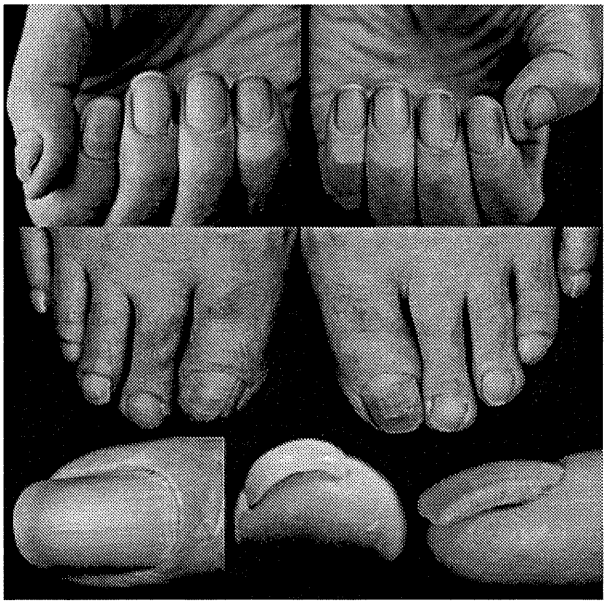

Figure 1. Clinical findings. The fingernails and toenails show yellowish discoloration, thickening, increased curvature and absent lunulae.

Correspondence: Riichiro Abe, M.D., Department of Dermatology, Hokkaido University Graduate School of Medicine, North 15 West 7, Kita-ku, Sapporo 060-8638, Japan. Email: aberi@med.hokudai.ac.jp

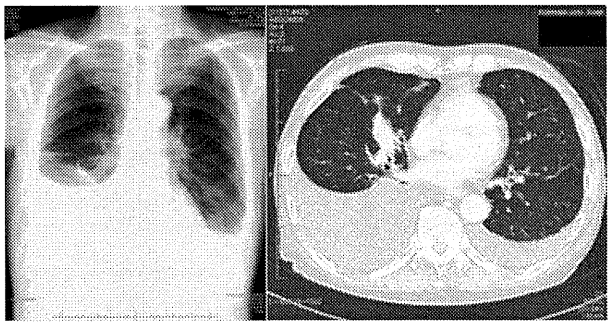

Figure 2. Bilateral pleural effusion. X-ray and computed tomography scans of the chest show bilateral pleural effusion.

infection) were excluded based on analysis of the pleural fluid. Diagnosis of YNS was made.

Yellow nail syndrome is characterized by the triad of yellow nails, lymphedema and respiratory manifestations. The presence at any given time of one of these three manifestations is sufficient to establish the diagnosis.[1] Characteristic nail features in YNS seem to be the most variable finding and the first to be recognized.[6] We questioned whether there are other manifestations suggesting YNS when we found yellow discoloration of the nails. The complete triad, which was seen in our case, is observed in only approximately 23.4% of YNS patients.[7]

Many conditions have been associated with YNS, particularly respiratory manifestations, such as bronchiectasis and recurrent lower respiratory tract infection, which are present in approximately half of the patients.[8] Other conditions with YNS include immunodeficiency states,[6] connective tissue diseases, and several malignancies, such as breast cancer[3] and lymphoproliferative disorders.[4] Rheumatoid arthritis is the autoimmune disease that is most commonly associated with YNS.[5]

The pathogenesis of the YNS manifestations is unknown. Recent studies have suggested that microvasculopathy with protein leakage may be more likely than functional lymphatic insufficiency as an explanation for the etiology of YNS.[8] The characteristic discoloration of the nails may be due to accumulation of lipofuscin, which is the product of fatty acid oxidation in the nail plate.[9] Another suggestion is that there are melanin particles in the nails, which become apparent when the nail matrix becomes inflamed.

Although there are no established effective treatments for the nail manifestations, partial or complete improvement occurs spontaneously in up to one-third of patients.[5] Some cases were reported to improve with better control of the respiratory manifestations.[6] Another paper reported that the nails returned to normal when a complicated tumor regressed.[3] Therefore, yellow nails may be an indicator of other coexistent manifestations of YNS or complications. In our case, worsening of the nail manifestations might be associated with the severity of lymphedema or pleural effusion.

The manifestations seen in YNS are not necessarily coincidental. When a patient clinically shows yellow nails, we should carefully consider YNS and conduct follow ups for any complications.

Inkin HAYASHI, Riichiro ABE, Teruki YANAGI, Yukiko ABE, Hiroshi SHIMIZU

Department of Dermatology, Hokkaido University Graduate School of Medicine, Hokkaido University, Sapporo, Japan

REFERENCES

1 Samman PD, White WF. The 'yellow nail' syndrome. *Br J Dermatol* 1964; **76**: 153–157.
2 D'Alessandro A, Muzi G, Monaco A *et al.* Yellow nail syndrome: does protein leakage play a role? *Eur Respir J* 2001; **17**: 149–152.
3 Iqbal M, Rossoff LJ, Marzouk KA, Steinberg HN. Yellow nail syndrome: resolution of yellow nails after successful treatment of breast cancer. *Chest* 2000; **117**: 1516–1518.
4 Siegelman SS, Heckman BH, Hasson J. Lymphedema, pleural effusions and yellow nails: associated immunologic deficiency. *Dis Chest* 1969; **56**: 114–117.
5 David-Vaudey E, Jamard B, Hermant C, Cantagrel A. Yellow nail syndrome in rheumatoid arthritis: a drug-induced disease? *Clin Rheumatol* 2004; **23**: 376–378.
6 Maldonado F, Tazelaar HD, Wang CW, Ryu JH. Yellow nail syndrome: analysis of 41 consecutive patients. *Chest* 2008; **134**: 375–381.
7 Nakielna EM. Yellow-nail syndrome: report of three cases. *Can Med Assoc J* 1976; **115**: 46–48.
8 Maldonado F, Ryu JH. Yellow nail syndrome. *Curr Opin Pulm Med* 2009; **15**: 371–375.
9 Cordasco EM Jr, Beder S, Coltro A *et al.* Clinical features of the yellow nail syndrome. *Cleve Clin J Med* 1990; **57**: 472–476.

Can end organ damage in scleroderma be predicted based on nail fold dermatoscopy findings?

Dear Editor,

Systemic scleroderma (SSc) is a connective tissue disease characterized by fibrosis and thickening of the skin. Decreased number of capillaries, dilated capillary loops and giant capillaries are frequently observed on nail fold examination.[1] Basillar pulmonary fibrosis, pulmonary arterial hypertension (PAH) and esophageal dysmotility are the most common comorbidities, and frequently cause SSc-related mortality.[2]

A total of 35 Turkish patients; 15 with diffuse cutaneous SSc (dcSSc) and 20 with limited cutaneous SSc (lcSSc), were

Correspondence: Sibel Dogan, M.D., Department of Dermatology, Faculty of Medicine, Hacettepe University, Sihhiye 06100, Ankara, Turkey. Email: sibel.dogan@hacettepe.edu.tr